

On the statistical analysis of grouped data: when Pearson χ^2 and other divisible statistics are not goodness-of-fit tests

Sara Algeri¹ and Estate V. Khmaladze²

¹ *School of Statistics, University of Minnesota, Minneapolis, MN, USA.*

Email: salgeri@umn.edu

² *School of Mathematics and Statistics, Victoria University of Wellington, Wellington, New Zealand.*

Email: estate.khmaladze@vuw.ac.nz

Summary. Thousands of experiments are analyzed and papers are published each year involving the statistical analysis of grouped data. While this area of statistics is often perceived – somewhat naively – as saturated, several misconceptions still affect everyday practice, and new frontiers have so far remained unexplored. Researchers must be aware of the limitations affecting their analyses and what are the new possibilities in their hands.

Motivated by this need, the article introduces a unifying approach to the analysis of grouped data, which allows us to study the class of divisible statistics – that includes Pearson’s χ^2 , the likelihood ratio as special cases – with a fresh perspective. The contributions collected in this manuscript span from modeling and estimation to distribution-free goodness-of-fit tests.

Perhaps the most surprising result presented here is that, in a sparse regime, all tests proposed in the literature are dominated by members of the class of weighted linear statistics.

Keywords: Goodness-of-fit, Divisible statistics, Grouped data, Counting experiments, small groups, Poisson statistics, Empirical processes, Distribution-free tests

1. Introduction

The rise of goodness-of-fit in statistics can be traced back to a correspondence between Edgeworth and Pearson at the end of the 19th century [cf. [Stigler, 1990](#)] on testing regarding the multinomial distribution of the 37 numbers on the roulette wheel, which led to Pearson’s seminal paper on the χ^2 -test [[Pearson, 1900](#)]. The latter can be considered one of the pillars of data analysis and, similarly to other foundational tools, it is still dominant in everyday practice.

Given K mutually exclusive groups or cells, labeled by x_k , let $\nu(x_k)$ be the frequencies observed in each group. Pearson’s χ^2 aims to test the hypothesis

$$H_0 : E[\nu(x_k)] = m_\theta(x_k) \quad \text{for all } k \in \{1, \dots, K\} \quad (1)$$

where the expected frequencies, $m_\theta(x_k)$, reflect our understanding of the phenomenon under study and may depend on a – possibly unknown – parameter $\theta \in \mathbb{R}^P$. The prescribed test statistic is

$$\sum_{k=1}^K \frac{(\nu(x_k) - m_\theta(x_k))^2}{m_\theta(x_k)},$$

and it is known to be χ^2 distributed under H_0 if $\min_{x_k} \{m_\theta(x_k)\} \rightarrow \infty$.

Following Pearson’s result, many different statistics have been introduced in the literature as substitutes to the χ^2 -test or supplementary to it [cf., [Cochran, 1952](#)]. They can be classified into two main kinds: those requiring the data to be in a grouped form and those that apply to continuous data.

Theoretical unification in the analysis of continuous data. An important feature of many goodness-of-fit statistics for continuous data is that they can be specified as functionals of the *empirical process*. Letting y_1, \dots, y_n be i.i.d. realizations of a real-valued random variable Y , distributed according to the distribution F , the empirical process $w_n(y)$ is such that

$$w_n(y) = \sqrt{n}[F_n(y) - F(y)],$$

with $F_n(y) = \frac{1}{n} \sum_{i=1}^n \mathbb{1}_{\{y_i \leq y\}}$ being the empirical distribution function. A prominent example of a goodness-of-fit test based on $w_n(y)$ is the Kolmogorov-Smirnov statistic [Kolmogorov, 1933, Smirnov, 1939]

$$\sup_y |w_n(y)|.$$

Also very prominent are the Cramer-von Mises [Smirnov, 1937] and Anderson-Darling [Anderson and Darling, 1954] statistics given by

$$\int w_n^2(y) dF(y) \quad \text{and} \quad \int \frac{w_n^2(y)}{F(y)(1-F(y))} dF(y),$$

respectively. Several other constructs used in the analysis of continuous data can be expressed as linear functionals of $w_n(y)$ [e.g., Wellner, 1992]. Such unification has led to notable advancements in different areas of statistics and has enabled developments in the theory and practice of goodness-of-fit, which continue at present [e.g., Henze and Meintanis, 2005, Khmaladze, 2016, Moscovich et al., 2016, Durio and Nikitin, 2016, Algeri, 2022, Dümbgen and Wellner, 2023, Roberts et al., 2023].

An attempt of unification in the analysis of grouped data. Alternatives to Pearson in the analysis of grouped data include the likelihood ratio

$$\sum_{k=1}^K \nu(x_k) \ln \frac{m_\theta(x_k)}{\nu(x_k)},$$

the linear statistic

$$\sum_{k=1}^K [\nu(x_k) - m_\theta(x_k)],$$

and the (cumulative) spectral statistic

$$\sum_{k=1}^K \mathbb{1}_{\{\nu(x_k) \leq q\}} \quad \text{with } q \in \mathbb{N},$$

which plays a central role in occupancy and diversity problems [e.g., Magurran, 1988, Mirakhmedov, 2007, Barbour and Gnedin, 2009, Khmaladze, 2011]. The commonality of these and many other tests is that they can all be expressed as the sum of a function of the observed and expected frequencies. They have been referred to in the literature as ‘divisible statistics’ (or sometimes ‘separable statistics’) [cf. Medvedev, 1970].

Given a function $g(z, t)$, usually differentiable in t , a divisible statistic based on such a function has the form

$$\frac{1}{\sqrt{K}} \sum_{k=1}^K g(\nu(x_k), m_\theta(x_k)). \quad (2)$$

The study of the class of divisible statistics as such began in the last quarter of the 20th century [e.g., Ivchenko and Medvedev, 1979, 1981, Khmaladze, 1984, Mnatsakanov, 1986, 1988]. Of particular interest is their behavior in the high-dimensional regime, also explored in recent literature on minimax optimal tests [e.g., Balakrishnan and Wasserman, 2018, 2019, Cai et al., 2024], in which the number of cells is not fixed and grows with the size of the sample.

Formally, letting $T = \sum_{k=1}^K m_\theta(x_k)$ be the expected sample size, we assume that K and T increase simultaneously so that

$$\frac{T}{K} \rightarrow c \in (0, \infty), \quad \text{as } T \rightarrow \infty \text{ and } K \rightarrow \infty, \quad (3)$$

and c can be interpreted as the average number of expected events per cell. Note that, differently from the case in which T grows at a faster rate than K , by assuming T and K have the same order of

magnitude, we allow the frequencies to be potentially small and, thus, not necessarily Gaussian in the limit. The condition in (3) is therefore necessary to describe many commonly encountered phenomena in which replicate observations are available, but only in a limited number. For example, in Edgeworth and Pearson’s epistolary communication, the roulette test relied on the normal approximation of the frequencies. This is sensible since the underlying distribution has 36 dimensions. But if we were to ask the same question today considering, instead of a roulette wheel, a poker machine with about 20 images on 15 wheels, this would give us $20^{15} \sim 10^{19}$ dimensions or cells, which could not be easily filled in any real experiment. In the statistical analysis of large texts, the asymptotic described by (3) is practically unavoidable. In a text composed of several hundred thousand words, more than 90% of the words that constitute its vocabulary are used no more than 10 times each, and about 50% of the words are used only once [e.g., Baayen, 2001]. In sociological surveys, the diversity of opinions is studied through questionnaires, and the situation is similar: in a questionnaire of, say, 15 binary questions, the number of different possible opinions, or groups, is $2^{15} \sim 33,000$. In a sample of 100,000 respondents, about 78% of different opinions will be expressed no more than 10 times; in balanced questionnaires, the probability of the answer ‘yes’ is close to 1/2 and c will be very close to 3 or 4 [e.g., Khmaladze, 2011]. The asymptotics in (3) are also typical in occupation problems in environmental ecology. In this field, most models involve a large number of different species populating a certain region. When an observational experiment is conducted over a given period of time, the number of different species observed is also large, but individuals from the same species may only be observed a handful of times [e.g., Magurran, 1988]. As discussed in detail below, the assumption in (3) is also relevant in counting experiments in physics and astronomy. In these and many other instances, researchers have so far been forced to group their data in large groups to use classical asymptotic theory in which c increases. This manuscript demonstrates that this grouping is not necessary. An asymptotic theory under (3) very much exists, although it is not the same theory as in the case in which the frequencies are accumulated.

The existing literature on the class of divisible statistics focuses on goodness-of-fit for simple hypotheses. One of the most notable results under (3) is that, if θ is known, no divisible statistic can detect all local departures from the null, somewhat invalidating their adequacy for goodness-of-fit. However, power can be restored by considering partial sums [cf. Khmaladze, 1984]. The effect of parameter estimation, on the other hand, has only been investigated on a case-by-case basis [cf., Cressie and Read, 1989] or for sub-classes such as that of power-divergence statistics [Cressie and Read, 1984, Müller and Osius, 2003]. No parametric result on the class of divisible statistics as a whole has yet been introduced, nor has an analog to the empirical process been proposed for the analysis of grouped data.

Divisible statistics anew: statistical motivation and relevance to the physical sciences.

The primary theoretical motivation of this manuscript is the need to unify the theory of statistical inference for grouped data to an extent comparable to what is enabled by the theory of empirical processes in the continuous regime. In Section 3, we show that it is possible to express different statistics involved in the analysis of grouped data as linear functionals based on the same random measure. This construction not only brings the desired unification but also unveils new phenomena, not visible in the analysis of i.i.d. observations. For example, a somewhat unanticipated result is presented in Section 6.4: in a sparse regime, all tests based on divisible statistics are dominated by weighted linear statistics.

In what follows, we assume the observed frequencies are independent Poisson random variables and (3) holds – that is, asymptotically, the frequencies remain Poisson and do not reach the Gaussian limit. We also assume that, given a compact subset of \mathcal{X} of \mathbb{R}^d with Lebesgue measure $|\mathcal{X}|$, the grouping leads to an exhaustive partition of \mathcal{X} into bins.

These assumptions are especially relevant in the physical sciences. Specifically, in physics and astronomy, the detector mechanism often leads to a discretization of the area under study. As a result, the data consists of event counts observed in the bins – be it channels, pixels, voxels, or other segments – of the discretized space. Moreover, even when the detector resolution is so high that it leads to a nearly continuous data stream, the statistical analysis is often conducted by partitioning the data into bins.

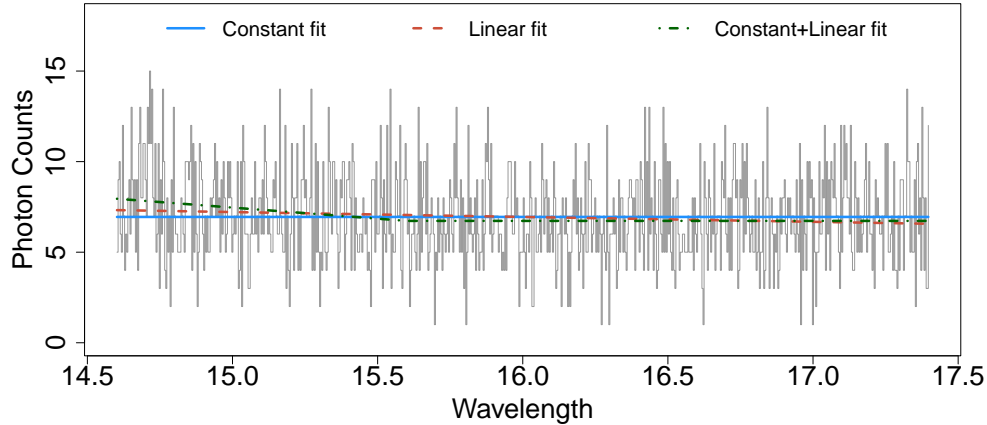


Fig. 1. *X*-ray source-free spectrum from a Chandra observation and discretized in 350 bins. The blue solid and red dashed lines are, respectively, the best fits obtained for constant, linear, and piecewise linear mean functions.

This choice may be dictated by the need for fast computations and numerical stability when fitting the models under study, to improve the signal-to-noise ratio, and/or to simplify the model assessment stage. In *X*-ray astronomy, for example, the images and the spectra collected by the Chandra *X*-ray Observatory [Swartz et al., 2010] are used to study the properties of celestial objects. In high-energy physics, the energy spectra produced by the Large Hadron Collider are at the core of searches for new physics beyond the Standard Model; of particular interest are thinly populated high-energy bins in which the new phenomena are often expected to appear [e.g., Belfonte et al., 2021]. In astroparticle physics, the images and the spectra generated by the Fermi Large Area Telescope [Atwood et al., 2009] enable the study of subatomic particles. In these settings, the data consists of Poisson-distributed photon counts observed over many bins. Hence, the goal is to estimate and validate the hypothesized mean function of a Poisson process defined over a discretized space.

Extensions to the multinomial scheme or situations in which the cells are defined by categorical variables are also possible in the proposed setup.

1.1. *An analysis of data from the Chandra X-ray observatory*

Throughout this manuscript, we consider data from the Chandra *X*-ray observatory to demonstrate the practical implications of our findings in scientific research and illustrate their implementation.

The Chandra *X*-ray Observatory is an *X*-ray telescope orbiting the Earth since its launch in 1999. It captures and probes *X*-rays from astronomical sources over a wide wavelength range. The analysis of *X*-ray spectra obtained with Chandra provides crucial information about the chemical composition, temperature, distance from the Earth, and other features of astronomical sources. In this manuscript, we consider an *X*-ray spectrum relevant to the study of RT Cru, a star belonging to a rare class of *X*-ray-emitting symbiotic systems. The origin of these systems remains poorly understood, making RT Cru a target of significant astronomical interest.

While previous studies made important contributions in the study of RT Cru [e.g., Luna and Sokoloski, 2007, Danehkar et al., 2020], many questions have remained unaddressed due to substantial background contamination in the 15 – 20 Å (Angstroms) range. In astronomy, the term ‘background’ refers to the combined signal of all astrophysical and cosmic sources, which are not those we aim to study. When analyzing data with significant background, accurate modeling of its distribution is crucial. For RT Cru, Zhang et al. [2023] conducted a comprehensive statistical analysis to validate and recalibrate proposed background models using ‘source-free spectra’ – that is, data collected in an off-source region of the detector. Our present analysis examines a subset of the data used in their study; it consists of a source-free spectrum in the 14.6 – 17.4 Å range. In this region, the hypothesized uniform

background model was rejected, and a linear correction for it was recommended. The analysis in this manuscript demonstrates the efficacy of the proposed methods in validating and complementing such findings.

Given the high resolution of the detector, the original dataset is unbinned; thus, in principle, one could attempt to perform an unbinned data analysis. However, the study of high-resolution X -ray spectra is typically conducted by binning the data [e.g., Luna and Sokolowski, 2007, Karovska et al., 2010, Bonamente, 2020]. Moreover, when analyzing low-resolution X -ray spectra, the data observed are naturally binned, with at least some of the bin counts being small. Keeping these aspects in mind, we choose to discretize the spectrum considered in 750 bins. As shown in Fig. 1, the bins average approximately seven counts, with many containing fewer than five counts. Such a choice allows us to demonstrate how the methods proposed in this manuscript can be used to test models for both low-resolution and sparsely binned high-resolution spectra while warning practitioners about their limitations.

2. Modeling framework

To formally define the quantities introduced in Section 1, consider a Poisson process $N_T(A)$, $A \subseteq \mathcal{X}$, with mean

$$E[N_T(A)] = T\Lambda_\beta(A) = T \int_A \lambda_\beta(x) dx, \quad (4)$$

where $\lambda_\beta(x)$ is the function describing the spatial spread of events over \mathcal{X} which depends on $\beta \in \mathbb{R}^{p-1}$. The parameter T determines the size of the sample – that is, in our context, ‘large samples’ means $T \rightarrow \infty$. It is reasonable to assume that $\lambda_\beta(x)$ is independent of T and

$$\int_{\mathcal{X}} \lambda_\beta(x) dx = 1 \quad \text{for all } \beta \in \mathbb{R}^{p-1}.$$

We also assume that λ_β is piece-wise continuous. Without loss of generality, let \mathcal{X} be a finite union of d -dimensional hypercubes. When the region of interest is not rectangular but merely a bounded set in \mathbb{R}^d , we can cover it with a finite union of cubes, \mathcal{R} , and assume $\lambda_\beta(x) = 0$ for all $x \in \mathcal{R} \setminus \mathcal{X}$. In other words, we can construct a grid on \mathcal{X} composed of K disjoint squares, or bins, denoted by $\{\Delta[x_k]\}_{k=1}^K$ and centered at points x_k . Assume all the bins have the same volume

$$\delta = \frac{|\mathcal{X}|}{K}.$$

The observed frequencies correspond to the increments of the process $N_T(A)$ over each bin, i.e.,

$$\nu(x_k) = N_T(\Delta[x_k]), \quad \text{for } k = 1, \dots, K,$$

where the dependence of $\nu(x_k)$ on T is dropped to simplify the notation. Their expectation is

$$m_\theta(x_k) = T \int_{\Delta[x_k]} \lambda_\beta(x) dx \sim T\delta\lambda_\beta(x_k) \sim c|\mathcal{X}|\lambda_\beta(x_k), \quad (5)$$

in which the first equivalence follows from the Lebesgue differentiation theorem [Rudin, 1987] and the second follows from (3). The collection of the frequencies $\{\nu(x_k)\}_{k=1}^K$, which, from some point of view, one would like to call a Poisson brush, is an unusual object. Indeed, $\nu(x_k)$ counts the number of jump points of N_T in the bin $\Delta[x_k]$; yet, as the bin shrinks, these points do not vanish because T increases at the same time; but where do the limiting jump points live? The answer is, we believe, associated with the notion of fold-up derivatives of shrinking sets and the local Poisson processes (cf. Khmaladze [2007], Khmaladze and Weil [2008]). However, we will not digress in this direction here.

In practice, β is often unknown or unspecified. Moreover, from a technical standpoint, it is convenient to treat T as an unknown parameter to be estimated, along with β . Since T may grow without limit, we estimate it in relative terms by considering $c \sim \frac{T}{K}$. Therefore, $\theta = (c, \beta)^\top \in \Theta \subseteq \mathbb{R}^p$ is the focus of estimation.

3. Divisible statistics as linear functionals based on the same random measure

As described in Section 1, classical goodness-of-fit statistics for testing (1) fall under the class of divisible statistics defined as in (2). This definition, however, does not include other important statistics encountered in the analysis of binned data, especially in the context of estimation.

To bring unification to the theory and broaden the class of divisible statistics, we propose a revision of its traditional definition to include any statistic that can be expressed as a linear functional of the random measure:

$$v_{\theta,K}(A, z) = \frac{1}{\sqrt{K}} \sum_{k=1}^K \mathbb{1}_{\{x_k \in A\}} \left[\mathbb{1}_{\{\nu(x_k) \leq z\}} - P(z|m_{\theta}(x_k)) \right], \quad A \subseteq \mathcal{X}, z \in \mathbb{N}. \quad (6)$$

in which $P(z|t)$ denotes the Poisson distribution function with mean t .

Let $m_{\theta}(x)$ be a step-wise constant function defined as

$$m_{\theta}(x) = m_{\theta}(x_k) \quad \text{for all } x \in \Delta[x_k]$$

and denote with $E_{\theta}[\cdot]$ the expectation taken with respect to a Poisson random variable, $\nu(x)$, with mean $m_{\theta}(x)$. From (5) it follows that $m_{\theta}(x)$ converges to $c|\mathcal{X}|\lambda_{\beta}(x)$. Consider now a more general class of divisible statistics with summands in (2) of the form $g_{\theta}(x_k, \nu(x_k)) = g(x_k, \nu(x_k), m_{\theta}(x_k))$ – that is, each term explicitly depend on the variable x_k . Hence, $g_{\theta}(x, z)$ constitutes the ‘inhomogenous’ version of $g(z, m_{\theta}(x))$. For example, when different weights are assigned to different bins, we may choose

$$g_{\theta}(x, z) = \omega(x)g(z, m_{\theta}(x)), \quad (7)$$

leading back to the ‘homogeneous’ divisible statistics in (2) when $\omega(x) = 1$. A divisible statistic defined by a function $g_{\theta}(x, z)$ is

$$v_{\theta,K}(g_{\theta}) = \iint g_{\theta}(x, z) v_{\theta,K}(dx, dz) = \frac{1}{\sqrt{K}} \sum_{k=1}^K \left[g_{\theta}(x_k, \nu(x_k)) - E_{\theta}[g_{\theta}(x_k, \nu(x_k))] \right], \quad (8)$$

where the integral is a random Stieltjes integral and $v_{\theta,K}(g_{\theta})$ is a direct analog of the function-parametric empirical process [e.g., [van der Vaart, 2000](#), Ch 19]. For instance, estimating equations are divisible statistics of the form in (8) equated to zero, and g_{θ} can be chosen as in (7), with $\omega(x)$ depending on θ . Partial sums can be constructed similarly by choosing $\omega(x) = \mathbb{1}_{\{x \in A\}}$. For fixed A and z , $v_{\theta,K}(A, z)$ is itself a divisible statistic, the localised (and centered) cumulative spectral statistic. It counts the number of bins in A with frequencies $\nu(x_k)$ less than or equal to z while centering the random terms, $\mathbb{1}_{\{\nu(x_k) \leq z\}}$, by their expectation.

The stochastic representation in (8) unfolds the intrinsic nature of all divisible statistics. Even those statistics that may at first appear highly non-linear – such as Pearson’s χ^2 – are, unavoidably, linear functionals of the random measure $v_{\theta,K}$. As demonstrated in Section 6, this inherent linear structure inhibits divisible statistics from performing goodness-of-fit testing.

To better understand the connection between the random measure $v_{\theta,K}$ and the classical empirical process for i.i.d. observations, rewrite (6) as

$$v_{\theta,K}(A, z) = \sqrt{K} \left[\frac{1}{K} \sum_{k=1}^K \mathbb{1}_{\{x_k \in A\}} \mathbb{1}_{\{\nu(x_k) \leq z\}} - \mu_{\theta,K}(A, z) \right] \quad (9)$$

with

$$\mu_{\theta,K}(A, z) = \frac{1}{K} \sum_{k=1}^K \mathbb{1}_{\{x_k \in A\}} P(z|m_{\theta}(x_k)) = \frac{\delta}{|\mathcal{X}|} \sum_{k=1}^K \mathbb{1}_{\{x_k \in A\}} P(z|m_{\theta}(x_k)).$$

In (9), the first average in k serves a purpose similar to that of the empirical distribution function. The expected value of such empirical distribution, given the collection of x_k , is the measure $\mu_{\theta,K}(A, z)$. The

latter assigns to each bin in A the Poisson probability $P(z|m_\theta(x_k))$. As $K \rightarrow \infty$, the marginal $\mu_{\theta,K}(A) = \mu_{\theta,K}(A, \infty)$ converges to $\mu(A) = |A|/|\mathcal{X}|$, the normalized Lebesgue measure, or uniform distribution, on \mathcal{X} and $\mu_{\theta,K}(A, z)$ converges weakly to

$$\mu_\theta(A, z) = \frac{1}{|\mathcal{X}|} \int_A P(z|m_\theta(x)) dx.$$

For example, as $K \rightarrow \infty$, we have

$$\iint g_\theta(x, z) \mu_{\theta,K}(dx, dz) = \int E_\theta[g_\theta(x, \nu(x))] \mu_K(dx) \rightarrow \iint g_\theta(x, z) \mu_\theta(dx, dz) = \int E_\theta[g_\theta(x, \nu(x))] \mu(dx).$$

The stochastic representation in (8) implies that – similarly to the i.i.d. setting in which classes of statistics can be expressed as values of function-parametric empirical processes [cf. [van der Vaart, 2000](#), Ch.19] – the class of divisible statistics becomes the function-parametric process based on $v_{\theta,K}$ in (6). The natural range for the functions g_θ indexing such a process is the Hilbert space

$$\mathcal{L}_2(\mu_{\theta,K}) = \{g_\theta(x, z) : \langle g_\theta, 1 \rangle = 0, \|g_\theta\| < \infty\}$$

with inner product $\langle g_\theta, g_\theta' \rangle = \iint g_\theta(x, z) g_\theta'(x, z) \mu_{\theta,K}(dx, dz)$ and norm $\|g_\theta\| = \sqrt{\langle g_\theta, g_\theta \rangle}$. The orthogonality condition $\langle g_\theta, 1 \rangle = 0$ indicates that we can restrict our attention to functions g_θ that are centered. Moreover, the representation in (8) and the central limit theorem imply that any divisible statistic is approximately Gaussian with variance $E_\theta[g_\theta^2] = \|g_\theta\|^2$. Seemingly different statistics, such as Pearson's χ^2 statistic and the spectral statistic, can be expressed as the values of the same function-parametric process $v_{\theta,K}(g_\theta)$. They are, therefore, not so different and are subject to the same treatment.

4. Divisible statistics with estimated parameters

When testing the validity of a given model $m_\theta(x)$ without a prescribed value of θ , one would need to replace the latter with an estimator. Therefore, it is useful to study how parameter estimation affects the structure of divisible statistics.

Let b_θ be a p -dimensional vector function with linearly independent components in $\mathcal{L}_2(\mu_{\theta,K})$ and consider the system of estimating equations

$$v_{\hat{\theta},K}(b_{\hat{\theta}}) = 0. \tag{10}$$

For example, when using Maximum Likelihood Estimation (MLE), b_θ is equal to the score function

$$\psi_\theta(x, z) = \frac{\partial}{\partial \theta} \ln p(z|m_\theta(x)) = \frac{\dot{m}_\theta(x)}{m_\theta(x)} (z - m_\theta(x)),$$

with $p(z|t)$ denoting the Poisson probability mass function with rate t and $\dot{m}_\theta(x) = \frac{\partial}{\partial \theta} m_\theta(x)$. When estimating θ via least squares, the minimization

$$\hat{\theta} = \arg \min_{\theta} \sum_{k=1}^K (\nu(x_k) - m_\theta(x_k))^2,$$

leads to $b_\theta(x, z) = -2\dot{m}_\theta(x)(z - m_\theta(x))$.

Under mild regularity conditions [e.g., [van der Vaart, 2000](#), Chapter 5], there exists a consistent root $\hat{\theta}$ of (10) and for this estimator the Taylor expansion

$$v_{\hat{\theta},K}(g_{\hat{\theta}}) = v_{\theta,K}(g_\theta) + \sqrt{K}(\hat{\theta} - \theta)^\top \frac{1}{\sqrt{K}} \frac{\partial}{\partial \theta} \iint g_\theta(x, z) v_{\theta,K}(dx, dz) + o_P(1)$$

is valid for $g_\theta \in \mathcal{L}_2(\mu_{\theta,K})$. Also, assume that the differentiation in θ can be moved under the integral sign and the coordinates of $\dot{g}_\theta(x, z) = \frac{\partial}{\partial \theta} g_\theta(x, z)$ belong to $\mathcal{L}_2(\mu_{\theta,K})$, then

$$\frac{1}{\sqrt{K}} \frac{\partial}{\partial \theta} \iint g_\theta(x, z) v_{\theta,K}(dx, dz) = \frac{1}{\sqrt{K}} v_{\theta,K}(\dot{g}_\theta) - \iint g_\theta(x, z) \frac{\partial}{\partial \theta} \mu_{\theta,K}(dx, dz)$$

in which the first term on the right-hand side is $o_p(1)$ and the second term is

$$\iint g_\theta(x, z) \frac{\partial}{\partial \theta} P(dz|m_\theta(x)) \mu_K(dx) = \int E_\theta [g_\theta(x, \nu(x)) \psi_\theta(x, \nu(x))] \mu_K(dx) = \langle g_\theta, \psi_\theta \rangle.$$

Therefore, the Taylor expansion above can be rewritten as

$$v_{\hat{\theta},K}(g_{\hat{\theta}}) = v_{\theta,K}(g_\theta) - \langle g_\theta, \psi_\theta^\top \rangle \sqrt{K}(\hat{\theta} - \theta) + o_P(1). \quad (11)$$

The components of b_θ live in $\mathcal{L}_2(\mu_{\theta,K})$, thus, the asymptotic representation in (11) can also be applied to the left-hand side of the estimating equations in (10). By equating the resulting expansion to zero, we obtain,

$$\sqrt{K}(\hat{\theta} - \theta) = \langle b_\theta, \psi_\theta^\top \rangle^{-1} v_{\theta,K}(b_\theta) + o_P(1) \quad (12)$$

and substituting the right-hand side of this equality into (11) gives

$$v_{\hat{\theta},K}(g_{\hat{\theta}}) = v_{\theta,K}(g_\theta) - \langle g_\theta, \psi_\theta^\top \rangle \langle b_\theta, \psi_\theta^\top \rangle^{-1} v_{\theta,K}(b_\theta) + o_P(1). \quad (13)$$

The leading term of the right-hand side involves values of $v_{\theta,K}$ at two functions, g_θ and b_θ . However, it is more natural and fruitful to view it as the value of $v_{\theta,K}$ at one function, Πg_θ , so that

$$v_{\theta,K}(\Pi g_\theta) = v_{\theta,K}(g_\theta) - \langle g_\theta, \psi_\theta^\top \rangle \langle b_\theta, \psi_\theta^\top \rangle^{-1} v_{\theta,K}(b_\theta)$$

where

$$\Pi g_\theta(x, z) = g_\theta(x, z) - \langle g_\theta, \psi_\theta^\top \rangle \langle b_\theta, \psi_\theta^\top \rangle^{-1} b_\theta(x, z). \quad (14)$$

According to Proposition 1, Π has a specific nature – it is a projector operator.

PROPOSITION 1. *The linear transformation in (14) is a projection of g_θ parallel to the function b_θ , which defines the estimating equations, and orthogonal to the score function ψ_θ , i.e.,*

$$\langle \Pi g_\theta, \psi_\theta \rangle = 0 \quad \text{and} \quad \Pi b_\theta(x, z) = 0. \quad (15)$$

The projector Π is orthogonal when $b_\theta = \psi_\theta$.

One can show that Π is a projection operator by verifying that $\Pi \Pi g_\theta = \Pi g_\theta$. The second equality in (15) tells us that b_θ belongs to the kernel of the operator Π . When $b_\theta \neq \psi_\theta$, however, the kernel of Π does not coincide with the orthogonal complement of its image. Hence, in general, the projection is not orthogonal, but, as noted in Proposition 1, it is when the parameters are estimated via MLE. For the latter, the leading term on the right-hand side of (13) can be expressed as

$$v_{\theta,K}(\Pi g_\theta) = v_{\theta,K}(g_\theta) - \sum_{j=1}^p \langle g_\theta, s_j \rangle v_{\theta,K}(s_j),$$

in which s_j denotes the j -th coordinate of the orthonormalized score function

$$s(x, z) = \langle \psi_\theta, \psi_\theta^\top \rangle^{-1/2} \psi_\theta(x, z)$$

and $\langle \psi_\theta, \psi_\theta^\top \rangle^{-1/2}$ is the inverse square root of the Fisher information matrix.

The existence of the projection operator Π , characterizing divisible statistics with estimated parameters, has implications of both practical and theoretical interest. For instance, as formalized in Proposition 4 in Section 6.1, it suggests that the random variable $v_{\theta,K}(\Pi g_\theta)$ should be stochastically smaller than $v_{\theta,K}(g_\theta)$, and thus, substituting $\hat{\theta}$ in $v_{\theta,K}$ changes the entire class of divisible statistics, making them stochastically smaller. It is also the key fact that enables the construction of distribution-free tests, with known asymptotic distribution, as described in Section 7.3. Moreover, $v_{\theta,K}(\Pi g_\theta)$ belongs to the class of divisible statistics defined by (8); hence, $v_{\hat{\theta},K}(g_{\hat{\theta}})$ is approximately Gaussian with mean zero and variance $\|\Pi g_\theta\|^2$.

Let us now choose the function b_θ defining the estimating equations in (10) equal to the right-hand side of (7) with the weighting function ω_θ depending on θ . That is, for a given choice of g , we consider the class of estimators defined by

$$v_{\hat{\theta},K}(\omega_{\hat{\theta}}g) = 0. \quad (16)$$

For instance, when g gives the linear statistic, two members of such a class are the MLE and the least squares estimator with $\omega_\theta(x) = \frac{\dot{m}_\theta(x)}{m_\theta(x)}$ and $\omega_\theta(x) = -2\dot{m}_\theta(x)$, respectively.

The estimator with the minimum variance among those given by (16) can be constructed by choosing $\omega_\theta(x)$ equal to

$$\gamma_\theta(x) = \frac{E_\theta[g(\nu(x), m_\theta(x))\psi_\theta(x, \nu(x))]}{E_\theta[g^2(\nu(x), m_\theta(x))]} \quad (17)$$

This result is formalized in Proposition 2.

PROPOSITION 2. *Let $\hat{\theta}$ be a consistent root of the estimating equations defined in (16) and let u be a vector in \mathbb{R}^p . For a given choice of g , the asymptotic variance of $u^\top \sqrt{K}(\hat{\theta} - \theta)$ is the smallest when $\omega_\theta = \gamma_\theta$.*

PROOF. By the definition of γ_θ we have that $\langle \omega_\theta g, \psi_\theta^\top \rangle = \langle \omega_\theta g, g\gamma_\theta^\top \rangle$. Therefore, the asymptotic representation of $\hat{\theta}$ is

$$\sqrt{K}(\hat{\theta} - \theta) \sim \langle \omega_\theta g, g\gamma_\theta^\top \rangle^{-1} v_{\theta,K}(\omega_\theta g). \quad (18)$$

Let us now consider the random variables

$$V = u^\top \langle \omega_\theta g, g\gamma_\theta^\top \rangle^{-1} v_{\theta,K}(\omega_\theta g) \quad \text{and} \quad W = u^\top \langle \gamma_\theta g, g\gamma_\theta^\top \rangle^{-1} v_{\theta,K}(\gamma_\theta g).$$

After some algebra, we obtain that their covariance is $E_\theta[VW] = E_\theta[W^2]$. Hence,

$$0 \leq E_\theta[(V - W)^2] = E_\theta[V^2] - E_\theta[W^2];$$

thus, the variance of W is always smaller or equal to that of V . \square

When g defines the linear statistic, we have that $\gamma_\theta g = \psi_\theta$. When g is not linear, for each x fixed, $\gamma_\theta g$ gives the best mean-square approximation of ψ_θ given g . For example, when g defines the centred Pearson's χ^2 statistic, $\gamma_\theta g$ specifies as

$$\frac{\dot{m}_\theta(x)}{2m_\theta(x) + 1} \left[\frac{(z - m_\theta(x))^2}{m_\theta(x)} - 1 \right],$$

and for the centred spectral statistic, $\gamma_\theta g$ is

$$\frac{q - m_\theta(x)}{1 - p(q|m_\theta(x))} \frac{\dot{m}_\theta(x)}{m_\theta(x)} [\mathbb{1}_{\{z \leq q\}} - P(q|m_\theta(x))].$$

In real-data analyses, statisticians would typically choose a function g for goodness-of-fit testing, and, in some instances, they may also want to, or have to, use the same function to estimate the unknown parameters. For instance, in the so-called problem of empty boxes, $q = 0$, one has only information of which boxes are empty; the frequencies $\{\nu(x_k)\}_{k=1}^K$ are not available [see, e.g., Gnedin et al., 2007, Domanski, 2012]. Yet, an estimation of the parameters is needed. What should be the form of the estimating equations? – Proposition 2 provides the answer. Nonetheless, as shown in Section 6.1, when applicable, the MLE is preferable for goodness-of-fit.

4.1. Testing background uniformity in sparse X-ray spectra via Pearson's χ^2 test

In the analysis of source-free X-ray spectra, the mean function is often assumed to be constant [e.g., Luna and Sokolowski, 2007, Bonamente, 2020], that is, $m_\theta(x)$ is identically equal to c for all $x \in \mathcal{X}$. In this setting, the score function is $\psi_\theta(x, z) = \frac{1}{c}(z - c)$ for all $x \in \mathcal{X}$; thus, when c is estimated via MLE, we obtain $\hat{c} = \frac{\sum_{k=1}^K \nu(x_k)}{K}$.

The divisible statistic $v_{\hat{\theta}, K}(g_{\hat{\theta}})$ chosen to test the hypothesis of uniformity of the background is the centered Pearson's statistic, i.e.,

$$\frac{1}{\sqrt{K}} \sum_{k=1}^K \left[\frac{(\nu(x_k) - \hat{c})^2}{\hat{c}} - 1 \right];$$

hence, $g_\theta(x, z) = \frac{(z-c)^2}{c} - 1$ for all $x \in \mathcal{X}$. Moreover,

$$\|\psi_\theta\|^2 = \frac{1}{c}, \quad s(x, z) = \frac{(z-c)}{\sqrt{c}}, \quad \|g_\theta\|^2 = 2 + \frac{1}{c}, \quad \text{and} \quad \langle g_\theta, s \rangle = \frac{1}{\sqrt{c}}.$$

The theoretical results in Section 4 imply that when the number of bins considered is sufficiently large, the asymptotic null distribution of Pearson's statistic is Gaussian with zero mean and variance $\|g_\theta\|^2 - \langle g_\theta, s \rangle^2 = 2$.

Let us now test the hypothesized uniformity of the background density using the source-free spectrum from Chandra in Fig. 1. For these data, $\hat{c} = 6.947$, and the value of the Pearson's χ^2 statistic observed is -0.852 . The p-value based on the Gaussian approximation is 0.547. Thus, the test completely fails to reject the constant background model. This result is in contrast with the recommendation provided by Zhang et al. [2023]. In their study, the authors tested the same hypothesis by means of smooth tests [cf. Lehmann and Romano, 1986, Chapter 16]. Their approach resulted in a rejection of the uniform assumption and proposed the introduction of an additional linear term to suitably model the mean function of the spectrum. The divergence in conclusions, however, is not surprising and, as we shall see in Section 6.3, can be formally explained from a theoretical standpoint: Pearson's χ^2 and many other divisible statistics have no power against weak departures from uniformity.

5. Contiguous alternatives and adequacy for goodness-of-fit

In the context of goodness-of-fit, the usual class of alternatives considered for such a study is that of *contiguous alternatives*. The notion of contiguity, introduced by Le Cam [1960], allows us to define sequences of alternatives that converge to the null hypothesis as the sample size increases, thereby describing local deviations from $m_\theta(x)$ due to fainter and fainter signals. Yet, these alternatives remain distinguishable from the null hypothesis.

Consider the distribution function $\Lambda_\beta(A) = \int_A \lambda_\beta(x) dx$. When θ is known, we say that

$$\tilde{m}_{\theta, T}(x) = m_\theta(x) \left[1 + \frac{h_T(x)}{\sqrt{T}} \right] \quad (19)$$

defines a sequence of *contiguous alternatives* to $m_\theta(x)$ if, for a given sequence of functions, $h_T \in L_2(\Lambda_\beta)$, we have

$$\limsup_{T \rightarrow \infty} \|h_T\|_{\Lambda_\beta}^2 = \limsup_{T \rightarrow \infty} \int h_T^2(x) \Lambda_\beta(dx) < \infty. \quad (20)$$

Moreover, if

$$\|h_T - h\|_{\Lambda_\beta}^2 \rightarrow 0, \quad \text{as } T \rightarrow \infty, \quad (21)$$

for some $h \in L_2(\Lambda_\beta)$, we say that $\tilde{m}_{\theta, T}(x)$ defines a sequence of *converging contiguous alternatives* to $m_\theta(x)$.

The function h defining a given sequence of alternatives can be interpreted as the functional direction from which $\tilde{m}_{\theta, T}(x)$ approaches $m_\theta(x)$ and $\|h\|_{\Lambda_\beta}^2$ can be taken equal to one without loss of essential

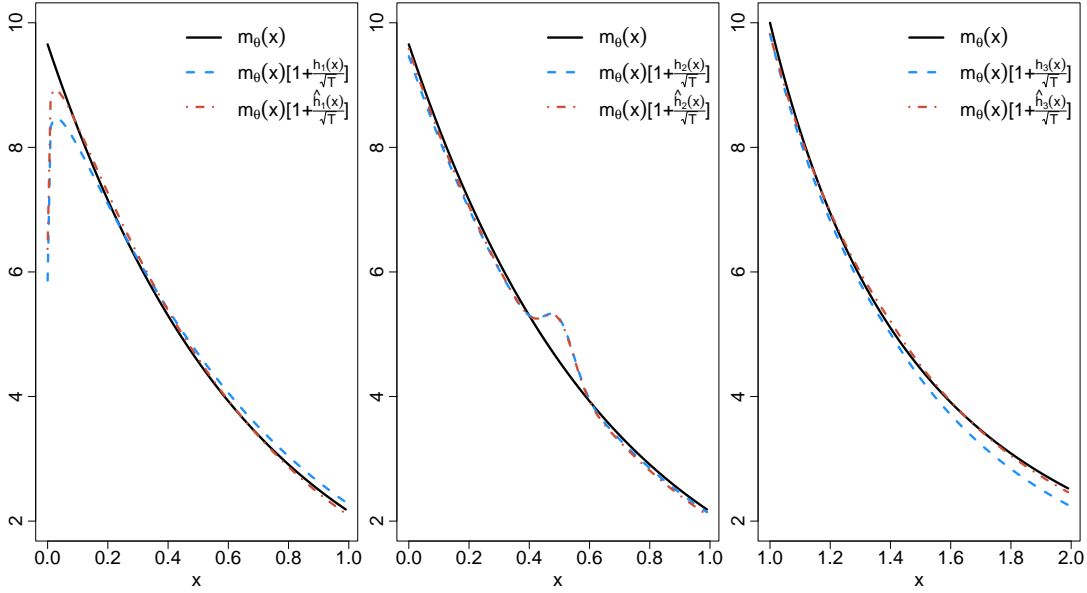


Fig. 2. Mean functions under the null (black solid lines), alternatives (blue dashed lines), and their component detectable by parametric tests obtained by replacing h in (19) with \hat{h} in (23) (red chained lines) for Example I (left panel), Example II (central panel), and Example III (right panel).

content. Sequences of $\tilde{m}_{\theta, \tau}(x)$ approaching $m_{\theta}(x)$ from the same direction can be considered equivalent and can be labeled by functions h in the unit ball in $L_2(\Lambda_{\beta})$.

When testing parametric hypotheses, the class of converging contiguous alternatives is much wider compared to the case of simple hypotheses. Such a class may seem to include all sequences of alternatives indexed by functions h in the unit ball in any of the spaces $L_2(\Lambda_{\beta})$, $\beta \in \mathbb{R}^{p-1}$. However, this is not quite true. Infinitesimal changes along the tangent spaces of the parametric family $\{\Lambda_{\beta}, \beta \in \mathbb{R}^{p-1}\}$ are now not relevant. As the projection argument of Proposition 1 and Proposition 4 in Section 6.1 show, such changes are not detectable by statistics with estimated parameters. More specifically, we will consider alternatives satisfying the conditions

$$\int h(x) \Lambda_{\beta}(dx) = 0 \quad \text{and} \quad \int h(x) \frac{\dot{\lambda}_{\beta}(x)}{\lambda_{\beta}(x)} \Lambda_{\beta}(dx) = 0, \quad (22)$$

with $\dot{\lambda}_{\beta}(x) = \frac{\partial}{\partial \beta} \lambda_{\beta}(x)$. The first condition excludes sequences of alternatives that differ from $\lambda_{\beta}(x)$ only by a scaling factor and can be accounted for through the estimation of c . In other words, we consider alternatives that only affect the spatial spread of the data over \mathcal{X} ; as a result, the product of $\lambda_{\beta}(x)$ and the term in the square brackets in (19) integrates to one. The second condition in (22) excludes alternatives indexed by functions $h \in L_2(\Lambda_{\beta})$ which are linear combinations of the coordinates of $\frac{\dot{\lambda}_{\beta}(x)}{\lambda_{\beta}(x)}$. The latter describes small changes in $\lambda_{\beta}(x)$ in β [cf. Amari, 1985, Kass and Vos, 2011]. Such deviations do not describe departures from the parametric family as such and are incorporated into the null through the estimation of β . Alternatives for which both conditions in (22) hold are of the form

$$\hat{h}(x) = h(x) - \frac{\dot{m}_{\theta}(x)}{m_{\theta}(x)} \Gamma_{\theta}^{-1} \int \frac{\dot{m}_{\theta}(y)}{m_{\theta}(y)} h(y) \Lambda_{\beta}(dy), \quad (23)$$

with $\Gamma_{\theta} = \int \frac{\dot{m}_{\theta}(x)}{m_{\theta}(x)} \frac{\dot{m}_{\theta}(x)}{m_{\theta}(x)} \Gamma_{\theta} \Lambda_{\beta}(dx) = \frac{1}{c} \langle \psi_{\theta}, \psi_{\theta} \Gamma \rangle$. The three examples below illustrate how statistically interesting alternatives defined by functions h may differ from alternatives defined by functions \hat{h} and from the null hypothesis.

Example I. Let Λ_β be the distribution of an exponential random variable with rate $\beta = 1.5$ truncated over the range $\mathcal{X} = [0, 1]$. The function

$$h_1(x) = a \ln x + b,$$

corresponds to the normalized score function for the shape parameter of a (truncated) gamma distribution with the same rate β . It describes the direction from which the latter approaches our exponential model, whereas $a = 0.87$ and $b = 1.21$ ensure that h_1 has a unit norm. Hence, h_1 satisfies the first condition in (22) – that is, it affects the spatial spread of the data but has no impact on the expected sample size described by c .

The left panel of Fig. 2 shows the graphs of the models for the expected counts when $T = 500$ and $c = 5$. For this example, the alternative defined by h_1 (blue dashed line) and that given by \hat{h}_1 (red chained line) are somewhat different from one another. In this case,

$$\frac{\dot{\lambda}_\beta(x)}{\lambda_\beta(x)} = \varphi(\beta) - x \quad (24)$$

where $\varphi(\beta)$ is a constant depending on β . Thus, the component of h_1 collinear with (24) describes deviations within the family of exponential distributions; whereas, the component \hat{h}_1 , orthogonal to (24), involves a logarithmic term and describes what is truly of interest: deviations within the family of gamma distributions with shape parameter different from one.

Example II. In physics and astronomy, when a reliable description of the background is available, a common problem is the detection of a faint ‘bump-like’ signal on top of it. Assume the background density, $\lambda_b(x)$, to be the same truncated exponential null model described in Example I and let $\lambda_s(x, x_0)$ be the density of the signal, here assumed to be Gaussian with mean $x_0 = 0.5$ and standard deviation $\sigma = 0.05$. The density function for the alternative model, inclusive of both background and signal, is

$$(1 - \eta_T)\lambda_b(x) + \eta_T\lambda_s(x, x_0),$$

where $\eta_T \in \mathbb{R}$ is the signal strength relative to T – that is, the expected number of signal events is $T\eta_T$. Assume η_T to be appropriately small, i.e., $\eta_T = T^{-\frac{1}{2}}$. Hence, the alternative (background+signal) model defined by the above density can be rewritten as in (19), with $h_T(x)$ converging to

$$h_2(x) = a \left[e^{-\frac{1}{2} \left(\frac{x-x_0}{\sigma} \right)^2 + \beta x} - 1 \right]$$

in which the quantity in the square brackets corresponds to $\frac{\lambda_s(x, x_0)}{\lambda_b(x)} - 1$ and the constant $a = 0.44$ ensures that the function h_2 has a unit norm. Such a function describes the changes in the spatial spread due to the presence of the signal, whereas η_T quantifies the closeness of the null and the alternative models as a function of the sample size T , here set equal to 500.

The central panel of Fig. 2 shows that the alternatives defined by h_2 (blue dashed lines) and \hat{h}_2 (red chained line) overlap for almost all $x \in [0, 1]$. That is because, in this case, the part of h_2 collinear with (24), and responsible for deviations within the family of exponential distributions, is negligible.

Example III. Luminosity functions can often be described using power-laws and broken power-laws. Discerning between the two is a common problem arising in X-ray astronomy [e.g., Gladstone et al., 2009, Humphrey and Buote, 2004, Marlowe et al., 2014]. In statistical terms, a power-law is equal to a Pareto type I distribution, while a broken power-law can be constructed by introducing a cutpoint to induce a change in the slope. Let our null model correspond to a power-law with slope $\beta = 2$ and truncated over the interval $\mathcal{X} = [1, 2]$. The function

$$h_3(x) = a(\ln \xi - \ln x)\mathbb{1}_{\{x \geq \xi\}} + b$$

describes the direction from which a broken power-law with a cutpoint at $\xi = 1.4$ approaches the simple power-law model. Set $a = 5.58$ and $b = -0.40$ to ensure that h_3 has norm one. The right panel of Fig.

2 displays the graphs of the mean models under the null (black solid line), the alternatives defined by h_3 (blue dashed line), and \widehat{h}_3 (red chained line) when $T = 500$ and $c = 5$. In this example,

$$\frac{\dot{\lambda}_\beta(x)}{\lambda_\beta(x)} = \phi(\beta) - \ln x$$

where $\phi(\beta)$ is a constant depending on β . Comparing the above expression with that of h_3 , it is apparent that most of the departure from the null hypothesis entailed by \widehat{h}_3 consists of deviations within the parametric family. As a result, the statistically interesting part \widehat{h}_3 that remains unaffected by the estimation of β is rather weak and almost indistinguishable from the null.

In the literature, the use of contiguous alternatives typically requires the validity of (21). This condition is sufficient for contiguity but not necessary. On the contrary, (20) is both sufficient and necessary [cf. Oosterhoff and Van Zwet, 1979]. This implies that there exists a sub-class of alternatives that are contiguous even without (21). In this case, it is not possible to identify a direction from which $\widetilde{m}_{\theta,T}(x)$ approaches $m_\theta(x)$, and thus, the sequence of alternatives diverges or oscillates without limit around the null. These alternatives, interesting in themselves, cannot be detected via goodness-of-fit, neither in the continuous nor in the grouped data regime, but they remain discernible from the null through specifically adjusted empirical processes. For this reason, they have been called *chimeric alternatives* [cf. Khmaladze, 1998].

Therefore, in the attempt to formally define the adequacy of a statistical test for goodness-of-fit, we rely on the class of converging contiguous alternatives.

DEFINITION 1. (Adequacy for goodness-of-fit) *We say that a statistical test is adequate for goodness-of-fit if its power exceeds the significance level for all converging contiguous alternatives.*

While the expression ‘all converging contiguous alternatives’ is formally correct, given how these alternatives are defined, it may seem an exaggeration. Indeed, all the alternatives considered here preserve the assumption that the observed process is Poisson, i.e., a point process with independent increments. Thus, the statements under the null and the alternative only apply to the intensity of this process.

When testing simple hypotheses in a sparse regime, tests based on a single divisible statistic, including Pearson’s χ^2 , are known not to satisfy Definition 1 [cf. Khmaladze, 1984]. As shown in the sections that follow, the problem persists when testing parametric hypotheses.

In the remainder of the manuscript, we will only consider alternatives within the class of converging contiguous alternatives; thus, we will simply refer to them as ‘alternatives’.

6. On the behavior of divisible statistics under contiguous alternatives

6.1. Distribution of divisible statistics under converging contiguous alternatives

The stochastic representation of divisible statistics in (8) allows us to determine their power on the basis of the asymptotic behaviour of the shift they acquire under the alternatives. As noted in Section 3, the statistics $v_{\theta,K}(g_\theta)$ are asymptotically Gaussian with zero mean. The limits of their first two moments under the converging contiguous alternatives are given in Proposition 3.

PROPOSITION 3. *Denote with $\widetilde{E}_{\theta,T}[\cdot]$ and $\widetilde{V}_{\theta,T}[\cdot]$, respectively, the expectation and the variance taken under the assumption that each $\nu(x_k)$ has Poisson distribution with expected value $\widetilde{m}_{\theta,T}(x_k)$. Let h be the functional direction defining the alternatives as in (19) and (21). Then,*

$$\widetilde{E}_{\theta,T}[v_{\theta,K}(g_\theta)] \sim \frac{1}{\sqrt{c}} \int C(x; g_\theta) h(x) \mu(dx), \quad (25)$$

where

$$C(x; g_\theta) = E_\theta[g_\theta(x, \nu(x))(\nu(x) - m_\theta(x))]. \quad (26)$$

Moreover, $\widetilde{V}_{\theta,T}[v_{\theta,K}(g_\theta)] \sim \|g_\theta\|^2$.

PROOF. Recall that g_θ is assumed to be centered under the null. The expected value under the alternative is

$$\tilde{E}_{\theta,T}[v_{\theta,K}(g_\theta)] = \sqrt{K} \int \sum_{z=0}^{\infty} g_\theta(x, z) [p(z|\tilde{m}_{\theta,T}(x)) - p(z|m_\theta(x))] \mu_K(dx)$$

where the difference in the square bracket is asymptotically small because $\tilde{m}_{\theta,T}(x) - m_\theta(x)$ is asymptotically small, while the Poisson probabilities $p(z|t)$ are regular in t . Therefore, one can approximate it using

$$\begin{aligned} \sqrt{K} \frac{\partial p(z|m_\theta(x_k))}{\partial m_\theta(x_k)} (\tilde{m}_{\theta,T}(x_k) - m_\theta(x_k)) &= (z - m_\theta(x_k)) p(z|m_\theta(x_k)) \sqrt{K} \frac{\tilde{m}_{\theta,T}(x_k) - m_\theta(x_k)}{m_\theta(x_k)} \\ &= (z - m_\theta(x_k)) p(z|m_\theta(x_k)) \frac{1}{\sqrt{c}} h_T(x_k). \end{aligned} \quad (27)$$

The substitution of this approximation in the expression for $\tilde{E}_{\theta,T}[v_{\theta,K}(g_\theta)]$ leads to the result. (A formal justification of the approximation is given in the Supplementary Material.) As to the variance, the convergence $p(z|\tilde{m}_{\theta,T}(x)) \rightarrow p(z|m_\theta(x))$ implies

$$\tilde{V}_{\theta,T}[v_{\theta,K}(g_\theta)] = \int \tilde{E}_{\theta,T}[g_\theta(x, \nu(x)) - \tilde{E}_{\theta,T}[g_\theta(x, \nu(x))]]^2 \mu_K(dx) \rightarrow \int E_\theta[g_\theta^2(x, \nu(x))] \mu(dx) \sim \|g_\theta\|^2.$$

□

Since the asymptotic distribution of $v_{\theta,K}(g_\theta)$ under the alternatives differs from the null only in the mean, to assess the adequacy of divisible statistics for goodness-of-fit, we focus on their shift.

Assume that the representation in (13) is valid. According to Proposition 3, when $\hat{\theta}$ solves the estimating equations in (10), the limiting shift of $v_{\theta,K}(\Pi g_\theta)$ becomes

$$\tilde{E}_\theta[v_{\theta,K}(\Pi g_\theta)] \sim \frac{1}{\sqrt{c}} \int C(x; \Pi g_\theta) h(x) \mu(dx). \quad (28)$$

The analysis of when the right-hand side can be zero – and, therefore, of when tests based on $v_{\hat{\theta},K}(g_{\hat{\theta}})$ have no power – leads to four main findings. The first two are formalized in Proposition 4, the others will be discussed in Sections 6.3-6.4.

PROPOSITION 4. (i) *The limiting shift of $v_{\theta,K}(\Pi g_\theta)$ under sequence of alternatives defined by a function h is*

$$\tilde{E}_{\theta,T}[v_{\theta,K}(\Pi g_\theta)] \sim \frac{1}{\sqrt{c}} \int C(x; \Pi g_\theta) \hat{h}(x) \mu(dx), \quad (29)$$

with \hat{h} satisfying the conditions in (22). Thus, tangential deviations defined by the vector function $\frac{\hat{m}_\theta}{m_\theta}$ are, asymptotically, not detectable.

(ii) *If θ is estimated via MLE, the right-hand side of (29) reduces to*

$$\frac{1}{\sqrt{c}} \int C(x; g_\theta) \hat{h}(x) \mu(dx). \quad (30)$$

Moreover, if the asymptotic equality in (13) is valid, then for sequences of alternatives defined by a function \hat{h} , the limiting power of $v_{\hat{\theta},K}(g_{\hat{\theta}})$ is higher than or equal to that of $v_{\theta,K}(g_\theta)$.

PROOF. The projection nature of Πg_θ implies that, unlike $C(x; g_\theta)$, $C(x; \Pi g_\theta)$ is orthogonal to the vector function $\frac{\dot{m}_\theta}{m_\theta}$. Indeed, from the expression in (14) it follows that

$$\begin{aligned} C(x; \Pi g_\theta) &= C(x; g_\theta) - \langle g_\theta, \psi_\theta^\top \rangle \langle b_\theta, \psi_\theta^\top \rangle^{-1} C(x; b_\theta) \\ \text{where } \langle g_\theta, \psi_\theta^\top \rangle &= \int C(x; g_\theta) \frac{\dot{m}_\theta^\top(x)}{m_\theta(x)} \mu_\kappa(dx), \\ \langle b_\theta, \psi_\theta^\top \rangle &= \int C(x; b_\theta) \frac{\dot{m}_\theta^\top(x)}{m_\theta(x)} \mu_\kappa(dx), \end{aligned} \quad (31)$$

and $C(x; b_\theta)$ is a vector function. Therefore,

$$\int C(x; \Pi g_\theta) \frac{\dot{m}_\theta(x)}{m_\theta(x)} \mu_\kappa(dx) = 0.$$

At the same time, from (23) we have that the difference $h - \hat{h}$ is a linear combination of the coordinates of $\frac{\dot{m}_\theta}{m_\theta}$, and statement (i) follows.

When θ is estimated via MLE, according to Proposition 1, Π is an orthogonal projector parallel to the score function ψ_θ . Moreover,

$$\int C(x; \psi_\theta) \hat{h}(x) \mu(dx) \propto \int \frac{\dot{m}_\theta(x)}{m_\theta(x)} \hat{h}(x) \Lambda_\beta(dx) = 0.$$

Hence, for sequences of alternatives defined by a function \hat{h} , the limit of both $\tilde{E}_{\theta, T}[v_{\theta, \kappa}(g_\theta)]$ and $\tilde{E}_{\theta, T}[v_{\theta, \kappa}(\Pi g_\theta)]$ is equal to (30). Under the null hypothesis, the variance of $v_{\theta, \kappa}(\Pi g_\theta)$ is

$$\|\Pi g_\theta\|^2 = \|g_\theta\|^2 - \sum_{j=1}^p \langle g_\theta, s_j \rangle^2 \leq \|g\|^2$$

and, from Proposition 3, it is asymptotically equal to $\tilde{V}_{\theta, T}[v_{\theta, \kappa}(\Pi g_\theta)]$. Therefore, in the limit, the signal-to-noise ratio for $v_{\hat{\theta}, \kappa}(g_{\hat{\theta}})$ is greater than or equal to that of $v_{\theta, \kappa}(g_\theta)$ and, since both statistics are asymptotically Gaussian, statement (ii) follows. \square

As noted in Section 5, the first statement of Proposition 4 confirms that, when the parameters are estimated, only alternatives of the form in (23) can be detected by divisible statistics. The second statement suggests that, regardless of the choice of g_θ , even when θ is known, estimating it via MLE can lead to higher power against alternatives for which $h = \hat{h}$. One could easily quantify the power gain induced by MLE by relying on the Gaussian approximation of divisible statistics. The validity of Proposition 4 (ii) in finite samples will be illustrated through a numerical example in Section 6.4.

6.2. No single divisible statistic is adequate for goodness-of-fit

The limiting shifts in (25) and (28) are linear functionals in $L_2(\mu)$; hence, for any h lying in the subspaces of $L_2(\mu)$ annihilated by these functionals, the limiting power will be equal to the significance level.

For instance, for the (centered) Pearson's χ^2 statistic :

$$\frac{1}{\sqrt{K}} \sum_{k=1}^K \frac{(\nu(x_k) - m_\theta(x_k))^2}{m_\theta(x_k)} - 1, \quad (32)$$

we have that $C(x; g_\theta) = 1$ for all $x \in \mathcal{X}$. Hence, when θ is estimated via MLE, the shift in (30) reduces to

$$\frac{1}{\sqrt{c}} \int \hat{h}(x) \mu(dx). \quad (33)$$

Therefore, Pearson's χ^2 has no power against alternatives approaching the null from a direction \widehat{h} orthogonal to one with respect to the Lebesgue measure. Equation (33) also implies that no departures from uniformity can be detected by Pearson's statistic, a problem originally pointed out by Chibisov [1965]. Unfortunately, this fallacy is not limited to the case of Pearson's χ^2 but, as demonstrated in Section 6.3, it affects an entire subclass of divisible statistics.

Examples I-III (continued). When c and β are estimated via MLE, for all three examples, the power of Pearson's χ^2 , obtained by means of 100,000 Monte Carlo replicates, is approximately equal to the significance level, here chosen to be 5%. While unpleasant, this result has a clear theoretical explanation. As noted above, when the parameters are estimated, only the alternatives defined by the functions \widehat{h}_j , $j = 1, 2, 3$ (red chained lines in Fig. 2) are detectable by divisible statistics. In Example III, the effect of \widehat{h}_3 is rather faint. Thus, regardless of the choice of g_θ , no divisible statistic is likely to detect such a deviation. On the other hand, both alternatives defined by \widehat{h}_1 and \widehat{h}_2 in Examples I and II are distinguishable from the null. When using Pearson's χ^2 , however, the limiting shift is approximately equal to -0.014 in Example I and -0.019 in Example II. This tells that, despite \widehat{h}_j , $j = 1, 2$ being not so small, their integrals are. Thereby leading to a loss of power.

Note that, although divisible statistics do not satisfy Definition 1, there exist situations in which scientists may be willing to sacrifice adequacy for goodness-of-fit to ensure high power against at least some classes of alternatives relevant to a given application. In the construction of such tests, the structure of the shift in (28) can be used to verify that, for a given choice of g_θ , power is preserved in the directions defining such alternatives.

6.3. On the impossibility of testing uniformity via space-homogeneous divisible statistics

In the previous sections, we saw some implications of the fact that the shift of $v_{\widehat{\theta,K}}(g_{\widehat{\theta}})$ is a linear functional from \widehat{h} . In particular, from Proposition 4 (i), we have that this linear functional is not defined by the function g_θ but by $C(x; \Pi g_\theta)$. This leads to a phenomenon that does not have an analogy in the classical theory of empirical processes. What can now occur is the following: a non-zero function g_θ produces a non-zero divisible statistic, but if $C(x; \Pi g_\theta) = 0$ for all $x \in \mathcal{X}$, then the shift of this statistic is zero for all alternatives.

One situation in which this phenomenon arises is when $v_{\theta,K}(g_\theta)$ belongs to the class of *space-homogeneous* divisible statistics defined as follows.

DEFINITION 2. *We say that $v_{\theta,K}(g_\theta)$ is a space-homogeneous divisible statistic, if the function $C(x; g_\theta)$ in (26) is constant.*

For example, regardless of the model being tested, both the (centered) Pearson's statistic and the statistic

$$\frac{1}{\sqrt{K}} \sum_{k=1}^K \left[\frac{\nu(x_k)}{m_\theta(x_k)} - 1 \right]$$

are space-homogeneous.

When λ_β is uniform, the class of space-homogeneous statistics is rather broad. In this case, the frequencies $\{\nu(x_k)\}_{k=1}^K$ are all identically distributed Poisson random variables with mean $m_\theta(x_k) = c$ for all $k = 1, \dots, K$. Therefore, if $g_\theta(\nu(x_k), m_\theta(x_k)) = g(\nu(x_k), c)$ does not depend on x_k explicitly, then these random variables are also identically distributed for all $k = 1, \dots, K$ and thus $C(x; g_\theta)$ is constant. This brings us to the following statement:

PROPOSITION 5. *Suppose λ_β is the uniform density on \mathcal{X} and c is estimated with MLE. Then, for any space-homogeneous divisible statistics,*

$$\widetilde{E}_{\theta,T}[v_{\theta,K}(\Pi g_\theta)] \sim 0,$$

that is, no such statistic has any asymptotic power for any h .

PROOF. Since $C(x; g_\theta)$ is constant and $\lambda_\beta(x) = |\mathcal{X}|^{-1}$ for all $x \in \mathcal{X}$, we have

$$C(x; \Pi g_\theta) = C(x; g_\theta) - \int C(x; g_\theta) \mu_K(dy) = 0.$$

It follows that, for any h , the limiting shift in (28) is zero. \square

Proposition 5 tells us that, although uniformity is a relevant null hypothesis in many practical settings, no space-homogeneous statistic is useful for detecting departures from it.

6.3.1. Space-homogeneous statistics are unsuitable to test constant background in X-ray spectra

When analyzing the source-free X-ray spectrum from Chandra introduced in Section 4.1, Pearson's statistic failed to reject the hypothesis of a constant background model. As a follow-up study, consider the weighted linear statistic

$$\frac{1}{\sqrt{K}} \sum_{k=1}^K \frac{\nu(x_k) - m_\theta(x_k)}{m_\theta(x_k)}; \quad (34)$$

and the (centered) likelihood ratio – known in astronomy as ‘Cash statistic’ [Cash, 1979] – defined by the function

$$g_\theta(x, z) = z \ln z - E_\theta[\nu(x) \ln \nu(x)] - (z - m_\theta(x))(1 + \ln m_\theta(x)).$$

The importance of (34) will be discussed in the next section. When testing the hypothesis $H_0 : m_\theta(x) = c$, the p-values obtained by means of a parametric bootstrap simulation involving 100,000 replicates are 0.145 for the weighed linear statistic and 0.987 for the likelihood ratio. As expected, neither statistic rejected the constant background model. We argue that, in this specific application, the deviations of the true background model from uniformity are indeed contiguous and, therefore, undetectable by space-homogeneous divisible statistics. Nevertheless, as shown in Section 7.1, they can be detected when relying on omnibus functionals of the process involving their partial sums.

6.4. Every divisible statistic is dominated by a weighted linear statistic.

The situation in which $C(x; \Pi g_\theta)$ is identically equal to zero for non-zero choices of g_θ can be retrieved in most settings, not only in the case of space-homogeneous statistics.

To see how this can happen, consider the structure of the projection operator in (14). At first glance, choosing g_θ orthogonal to the score function – i.e., such that $\langle g_\theta, \psi_\theta \rangle = 0$ – may seem advantageous: for all such g_θ , $\Pi g_\theta = g_\theta$, thus, statistics $v_{\hat{\theta}_K}(g_\theta)$ will be asymptotically equivalent to $v_{\theta_K}(g_\theta)$ and, therefore, their asymptotic behaviour will not depend on whether we estimate θ or not. However, the condition $\langle g_\theta, \psi_\theta \rangle = 0$ is achieved as soon as $g_\theta(x_k, \nu(x_k))$ and $\nu(x_k)$ are uncorrelated for every given x_k , i.e.,

$$C(x_k, g_\theta) = E_\theta[g_\theta(x_k, \nu(x_k))(\nu(x_k) - m_\theta(x_k))] = 0,$$

which then leads to a zero limiting shift of the statistic $v_{\hat{\theta}_K}(g_\theta)$, making it useless. Let us understand the situation better. In particular, let us decompose a given g_θ into the parts orthogonal to and collinear with $\nu(x) - m_\theta(x)$:

$$g_\theta^\perp(x, z) = g_\theta(x, z) - \frac{C(x, g_\theta)}{m_\theta(x)}(\nu(x) - m_\theta(x)), \quad g_\theta^{\parallel}(x, z) = \frac{C(x, g_\theta)}{m_\theta(x)}(\nu(x) - m_\theta(x)). \quad (35)$$

Since $C(x, g_\theta^\perp) = 0$ for all $x \in \mathcal{X}$, unbinding $v_{\theta_K}(g_\theta)$ from the extra randomness due to $v_{\theta_K}(g_\theta^\perp)$ allows us to preserve the asymptotic shift while simultaneously reducing the variance. As formalized in Proposition 6, the same holds true when θ is estimated via MLE.

PROPOSITION 6. Assume that the asymptotic representation (13) is valid and θ is estimated via MLE. Then, for any divisible statistic $v_{\hat{\theta}_K}(g_\theta)$, there exists another divisible statistic, $v_{\hat{\theta}_K}(g_\theta^{\parallel})$, whose limiting power is greater than or equal to that of $v_{\hat{\theta}_K}(g_\theta)$.

PROOF. Recall that $v_{\hat{\theta}_K}(g_{\hat{\theta}})$ is asymptotically equivalent to $v_{\theta_K}(\Pi g_{\theta})$ and consider the expansion

$$v_{\theta_K}(\Pi g_{\theta}) = v_{\theta_K}(\Pi g_{\theta}^{\perp}) + v_{\theta_K}(\Pi g_{\theta}^{\parallel}).$$

From (31) it follows that, since $C(x_k; g_{\theta}^{\perp}) = 0$ for all x_k , we obtain $C(x_k, \Pi g_{\theta}^{\perp}) = 0$ for all x_k , regardless of the choice of b_{θ} defining the estimating equations in (10). This fact and Proposition 4 imply that $\tilde{E}_{\theta, T}[v_{\theta_K}(\Pi g_{\theta}^{\perp})] \sim 0$ for all alternatives. Therefore, $v_{\theta_K}(\Pi g_{\theta}^{\perp})$ will not be useful for testing purposes and $\tilde{E}_{\theta, T}[v_{\theta_K}(\Pi g_{\theta})]$ and $\tilde{E}_{\theta, T}[v_{\theta_K}(\Pi g_{\theta}^{\parallel})]$ have the same limit, i.e.,

$$\frac{1}{\sqrt{c}} \int C(x; \Pi g_{\theta}^{\parallel}) \hat{h}(x) \mu(dx) = \frac{1}{\sqrt{c}} \int C(x; g_{\theta}^{\parallel}) \hat{h}(x) \mu(dx),$$

where the equality follows from Proposition 4(ii). At the same time, from the equality in (14) we have $\Pi g_{\theta}^{\perp} = g_{\theta}^{\perp}$ and if θ is estimated via MLE, $b_{\theta} = \psi_{\theta}$ and Π is orthogonal, i.e., it is a self-adjoint projector. Therefore,

$$\langle \Pi g_{\theta}^{\perp}, \Pi g_{\theta}^{\parallel} \rangle = \langle \Pi^2 g_{\theta}^{\perp}, g_{\theta}^{\parallel} \rangle = \langle g_{\theta}^{\perp}, g_{\theta}^{\parallel} \rangle = 0.$$

Since Πg_{θ}^{\perp} and $\Pi g_{\theta}^{\parallel}$ are orthogonal, the limiting variance of $v_{\theta_K}(\Pi g_{\theta}^{\parallel})$ is

$$\|\Pi g_{\theta}^{\parallel}\|^2 = \|\Pi g_{\theta}\|^2 - \|\Pi g_{\theta}^{\perp}\|^2 \leq \|\Pi g_{\theta}\|^2.$$

Hence, the asymptotic power of $v_{\hat{\theta}_K}(g_{\hat{\theta}}^{\parallel})$ always exceeds or is equal to that of $v_{\hat{\theta}_K}(g_{\hat{\theta}})$, with equality holding when $g_{\theta} = g_{\theta}^{\perp}$ or $g_{\theta} = g_{\theta}^{\parallel}$. \square

Example IV. Let $K = 100$, $c = 5$, and $\lambda_{\beta}(x)$ is chosen to be a normal density truncated over the interval $\mathcal{X} = [0, 1]$ with mean β and variance $\sigma^2 = 0.04$. In this setup,

$$\frac{\dot{\lambda}_{\beta}(x)}{\lambda_{\beta}(x)} = \frac{x - \beta}{\sigma^2} - \int_0^1 \frac{x - \beta}{\sigma^2} \Lambda_{\beta}(dx)$$

and, assuming the true value of β to be 0.5, the integral on the right-hand side is zero. The functional direction defining the alternative is

$$h_4(x) = \frac{a}{2\sigma^2} \left[\left(\frac{x - \beta}{\sigma} \right)^2 - b \right];$$

for $a = 0.07$ and $b = 0.04$, it corresponds to the derivative of the log-likelihood of our (truncated) normal model taken with respect to σ^2 and orthonormalized with respect to the function identically equal to one in $L^2(\Lambda_{\beta})$. Since in a normal model the derivative of the log-likelihood with respect to the mean and the variance are orthogonal, we have $\int \frac{\dot{\lambda}_{\beta}(x)}{\lambda_{\beta}(x)} h_4(x) \Lambda_{\beta}(dx) = 0$; thus, the conditions in (22) are satisfied and $h_4 = \hat{h}_4$.

Consider the centered Pearson's χ^2 statistic in (32), for which $C(x_k; g_{\theta}) = 1$ for all x_k . Hence, the corresponding weighted linear statistic, $v_{\theta_K}(g_{\theta}^{\parallel})$, is given by (34). Under any alternative, these two statistics will have the same limiting shift, but the limiting variance of (34) is smaller. Begin with the case in which θ is known. For Pearson's χ^2 , the power estimated using 100,000 Monte Carlo replicates and choosing the significance level to be 5% is approximately 7.16%; whereas, for $v_{\theta_K}(g_{\theta}^{\parallel})$ the power is 10.53%. As expected, if we free ourselves from the extra randomness due to $v_{\theta_K}(g_{\theta}^{\perp})$, the power increases. When θ is estimated via MLE, the power of $v_{\hat{\theta}_K}(g_{\hat{\theta}}^{\parallel})$ amounts to 14.09% – that is, compared to Pearson's statistic with θ known, the use of g_{θ}^{\parallel} and estimation via MLE together lead to twice as much power.

Let us now consider the spectral statistic

$$\frac{1}{\sqrt{K}} \sum_{k=1}^K [\mathbb{1}_{\{\nu(x_k) \leq q\}} - P(q|m_{\theta}(x_k))], \quad \text{with } q \in \mathbb{R}, \quad (36)$$

for which $C(x; g_\theta) = -m_\theta(x)p(q-1|m_\theta(x))$; thus, $v_{\theta,K}(g_\theta'')$ specifies as

$$\frac{1}{\sqrt{K}} \sum_{k=1}^K p(q-1|m_\theta(x_k))(\nu(x_k) - m_\theta(x_k)). \quad (37)$$

Choose $q = 1$ and let the significance level be 5%. When θ is known, the simulated power of (36) obtained using 100,000 Monte Carlo replicates is 7.8% and amounts to 12.53% for the dominating weighted linear statistic in (37). When θ is estimated via MLE, the power is 13.49% – that is, when the information on the frequencies $\{\nu(x_k)\}_{k=1}^K$ is available and is incorporated into the analysis, it almost doubles the power of the classical spectral statistic.

7. Goodness-of-fit via divisible statistics

7.1. On the construction of goodness-of-fit tests based on partial sums

Despite the advantages given by parameter estimation against alternatives of the form in (23) and the use of g_θ'' in (35) to increase the power of single divisible statistics, neither of these phenomena guarantees their adequacy for goodness-of-fit. Nevertheless, power can be restored by relying on a family of divisible statistics.

As shown by Khmaladze [1984] for the case of simple hypotheses, one possible choice is the process of partial sums

$$v_{\theta,K}(g_\theta \mathbb{1}_A) = \int_A \int g_\theta(x, z) v_{\theta,K}(dx, dz) = \frac{1}{\sqrt{K}} \sum_{x_k \in A} g_\theta(x_k, \nu(x_k)), \quad (38)$$

in which $g_\theta \mathbb{1}_A$ denotes functions of the form $g_\theta(x, z) \mathbb{1}_{\{x \in A\}}$. When testing parametric hypotheses, the process of interest is

$$v_{\theta,K}(g_\theta \mathbb{1}_A) = v_{\theta,K}(\Pi g_\theta \mathbb{1}_A) + o_P(1) \quad (39)$$

in which the functions $\Pi g_\theta \mathbb{1}_A$ can be written explicitly as

$$\Pi g_\theta(x, z) \mathbb{1}_{\{x \in A\}} = g_\theta(x, z) \mathbb{1}_{\{x \in A\}} - \langle g_\theta \mathbb{1}_A, \psi_\theta^\top \rangle \langle b_\theta, \psi_\theta^\top \rangle^{-1} b_\theta(x, z).$$

In this paper, we choose the sets A to be members of the *scanning family* [cf. Khmaladze, 1993], i.e., an increasing sequence of subsets, $\mathcal{A} = \{A_t\}_{0 \leq t \leq 1}$, of \mathcal{X} such that

- (a) $A_s \subseteq A_t$ if $s \leq t$;
- (b) $|A_0| = 0, |A_1| = |\mathcal{X}|$;
- (c) $|A_t|$ is absolutely continuous in t .

It follows that one can label the functions in $\mathcal{L}_2(\mu_{\theta,K})$ indexing the processes in (38)-(39) using the one-dimensional time parameter $t \in [0, 1]$. As shown in Section 7.3, this also simplifies the construction of asymptotically distribution-free goodness-of-fit tests.

The process $v_{\theta,K}(g_\theta \mathbb{1}_A)$ consists of partial sums of independent random variables; hence, it converges weakly to a Brownian motion [cf. Pyke, 1983, Kenneth and Pyke, 1986]. The projection $v_{\theta,K}(\Pi g_\theta \mathbb{1}_A)$, on the other hand, converges weakly to a projected Brownian motion. Under the null, the mean function of such processes is identically equal to zero for all $A \in \mathcal{A}$; whereas their shift under the alternatives can be derived by replacing g_θ with $g_\theta \mathbb{1}_A$ in (25) and (28). For instance, (25) becomes

$$\frac{1}{\sqrt{c}} \int_A C(x; g_\theta) h(x) \mu(dx).$$

Since the integral is taken over all $A \in \mathcal{A}$, it is identically equal to zero only if $C(x; g_\theta) = 0$ for all $x \in \mathcal{X}$ or if the function h satisfies rather exotic conditions. Therefore, in practice, any choice of g_θ that differs from g_θ^\perp (cf. Section 6.4) would give a non-zero shift over at least one set $A \in \mathcal{A}$. Consequently,

goodness-of-fit tests satisfying Definition 1 can be constructed by considering omnibus functionals of the partial sum processes in (38)-(39) as test statistics.

For example, let us start with a collection of hyperrectangles

$$(-\infty, y_t] = (-\infty, y_{1t}] \times \cdots \times (-\infty, y_{dt}]$$

with $y_t = (y_{1t}, \dots, y_{dt}) \in \mathcal{X}$ such that, if $s \leq t$, $y_{is} \leq y_{it}$, for all $i = 1, \dots, d$. Then choose A_t to be $(-\infty, y_t] \cap \mathcal{X}$. A possible test statistic for parametric goodness-of-fit is

$$\widehat{KS} = \max_t |v_{\widehat{\theta, K}}(g_{\widehat{\theta}}^{\prime\prime} \mathbb{1}_t)| \quad (40)$$

in which $\mathbb{1}_t$ denotes the indicator function $\mathbb{1}_{\{x \in (-\infty, y_t] \cap \mathcal{X}\}}$ and $g_{\widehat{\theta}}^{\prime\prime}$ is constructed as in (35). The statistic in (40) is the Kolmogorov-Smirnov statistic for testing parametric hypotheses in the binned data regime.

Example IV (continued). Consider the \widehat{KS} statistics given by the maxima of the cumulative sums of the summands of the divisible statistics in (34) and (37), i.e.,

$$\max_t \frac{1}{\sqrt{K}} \sum_{x_k \leq y_t} \frac{(\nu(x_k) - m_{\widehat{\theta}}(x_k))}{m_{\widehat{\theta}}(x_k)} \quad (41)$$

and

$$\max_t \frac{1}{\sqrt{K}} \sum_{x_k \leq y_t} p(q - 1 | m_{\widehat{\theta}}(x_k)) (\nu(x_k) - m_{\widehat{\theta}}(x_k))$$

with $y_t \in \{x_1, \dots, x_K\}$ and θ estimated via MLE. Under the same setup described in Section 6.4, such statistics have power 16.47% and 15.44%, respectively – approximately a 2% power increase compared to (34) and (37). However, we should not expect this result to be true in general. Specifically, a test based on functionals of the partial sums process should be preferred to a test based on a single divisible statistic – such as $v_{\widehat{\theta, K}}(g_{\widehat{\theta}}^{\prime\prime})$ – because the latter does not satisfy Definition 1. Nevertheless, it is possible that, for some alternatives, a single divisible statistic may exhibit higher power than functionals of the partial sums process.

7.1.1. On the detection of non-constant background shapes in X-ray source-free spectra

While in the analysis of X-ray spectra, contiguous departures from uniformity cannot be detected by space-homogeneous statistics (cf. Section 6.3), the results of Section 7.1 suggest that power can be retrieved through partial sums.

Considering the source-free Chandra spectrum described in Section 1.1, we tested the hypothesis of constant background using the \widehat{KS} statistic constructed as in (41) with $m_{\widehat{\theta}}(x_k) = \widehat{c}$, for all $k = 1, \dots, K$. A parametric bootstrap simulation with 100,000 replicates yielded a p-value of 0.008. Hence, at a 5% significance level, the uniform background assumption is rejected.

The same testing procedure has been implemented to test the linearity of $m_{\widehat{\theta}}(x)$. The linear mean function estimated via MLE is displayed as a red-dashed line in Figure 1. The bootstrap p-value obtained when testing such a model is 0.049, on the edge of being rejected at a 5% significance level.

While identifying a suitable model for this spectrum is beyond the scope of this manuscript, we tested a piecewise linear model comprising a linear function up to 15.6 Angstroms and remaining constant thereafter. The resulting fit is shown as a green-chained line in Figure 1. When considering the \widehat{KS} statistic in (41), the bootstrap p-value obtained amounts to 0.43. This indicates that introducing a breakpoint at 15.6Å to separate the constant and linear components may provide a better representation of the background distribution in the 14.6 – 17.4Å range than models previously proposed in the literature.

7.2. The projected parametric bootstrap

While the construction of asymptotically distribution-free tests for parametric hypotheses is possible (cf. Section 7.3), one can alternatively derive the null distribution of functionals of $v_{\widehat{\theta, K}}(g_{\widehat{\theta}}^{\prime\prime} \mathbb{1}_A)$ via

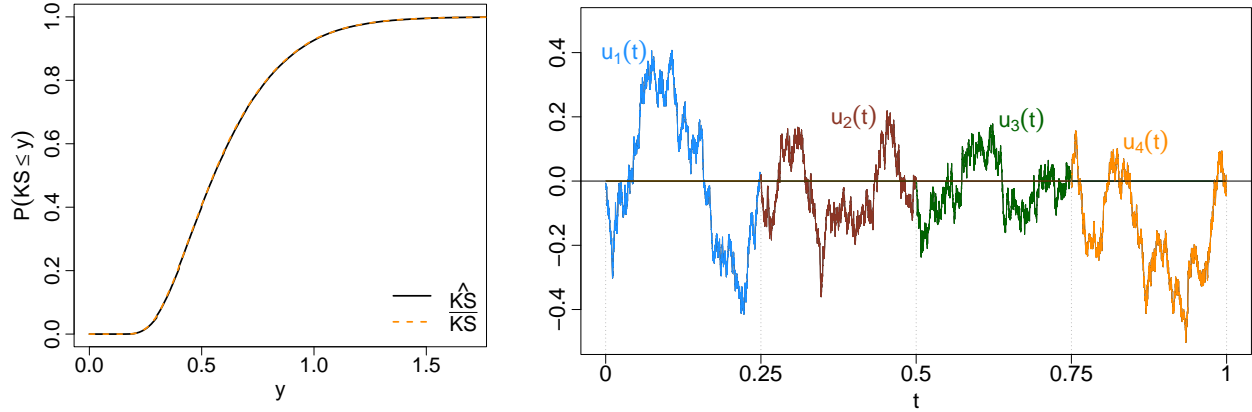


Fig. 3. Left Panel: Comparing the bootstrapped distribution of the Kolmogorov-Smirnov statistics \widehat{KS} and \overline{KS} , as defined in (40) and (43), using 100,000 replicates. Right panel: A realization of the limiting process of $v_{\theta,K}(U_p \Pi_r \ell_t)$ given by a succession of rescaled independent standard Brownian bridges, defined as in (47), when $p = 4$.

the parametric bootstrap. As discussed below, the computational effort required by the latter can be substantially reduced when relying on the projected process of partial sums.

Let us focus on the situation in which the process of partial sums is indexed by functions $g_\theta // \mathbf{1}_A$, and the parameters are estimated via MLE. Similar considerations can be made for any other choice of g_θ and other estimators solving the estimating equations in (10).

Denote with $\widehat{\theta}_{\text{obs}}$ the estimate of θ obtained via MLE on the set of data collected by the experiment. We are interested in simulating the null distribution of the process

$$v_{\widehat{\theta},K}(g_{\widehat{\theta}} // \mathbf{1}_A) = \frac{1}{\sqrt{K}} \sum_{x_k \in A} \frac{C(x_k; g_{\widehat{\theta}})}{m_{\widehat{\theta}}(x_k)} (\nu(x_k) - m_{\widehat{\theta}}(x_k)) \quad (42)$$

and its functionals. To account for the randomness associated with $\widehat{\theta}$, the classical parametric bootstrap entails maximizing the log-likelihood on each bootstrap sample and re-evaluating $v_{\widehat{\theta},K}(g_{\widehat{\theta}} // \mathbf{1}_A)$ at each bootstrap estimate of θ .

Let us now consider the projected process of partial sums

$$v_{\theta,K}(\Pi g_\theta // \mathbf{1}_A) = v_{\theta,K}(g_\theta // \mathbf{1}_A) - \sum_{j=1}^p \langle g_\theta // \mathbf{1}_A, s_j \rangle v_{\theta,K}(s_j).$$

Such a process is asymptotically equal to $v_{\widehat{\theta},K}(g_{\widehat{\theta}} // \mathbf{1}_A)$ (cf. Section 4), however, from a computational standpoint, simulating the null distribution of $v_{\theta,K}(\Pi g_\theta // \mathbf{1}_A)$ is more advantageous than simulating that of $v_{\widehat{\theta},K}(g_{\widehat{\theta}} // \mathbf{1}_A)$. That is because, in the former case, one needs not to re-estimate θ on each bootstrap sample. Instead, the randomness induced by parameter estimation is accounted for through the second term on the right-hand side of the above expression in which the inner products $\langle g_\theta // \mathbf{1}_A, s_j \rangle$ need only to be computed once at $\theta = \widehat{\theta}_{\text{obs}}$.

Numerical study. The computational benefits of the projected empirical process, particularly in the context of testing multivariate distributions in the i.i.d. setting, have been discussed in Algeri [2022]. To illustrate this aspect in the binned data regime, we rely on the setup of Example IV introduced in Section 6.4. We compare the bootstrapped null distribution of the Kolmogorov-Smirnov statistics in (40) with that of

$$\overline{KS} = \max_t |v_{\theta,K}(\Pi g_\theta // \mathbf{1}_t)|, \quad (43)$$

where t labels the sets $(-\infty, y_t] \cap \mathcal{X}$ (cf. Section 7.1) and g_θ'' is the function defining the statistic in (34). The results obtained are shown on the left panel of Fig. 3. Not surprisingly, the two bootstrapped distributions are effectively overlapping. The projected process $v_{\theta, \mathcal{K}}(\Pi g_\theta'' \mathbf{1}_t)$, however, provides substantial computational gain compared to $v_{\hat{\theta}, \mathcal{K}}(g_\theta'' \mathbf{1}_t)$. Specifically, simulating the null distribution of $\overline{\text{KS}}$ using 100,000 bootstrap replicates required only 5.51 seconds of (system+user) CPU time; approximately 3.3 times faster than simulating that of $\overline{\text{KS}}$ and which required 18.38 seconds of CPU time.

7.3. Asymptotically distribution-free goodness-of-fit tests via unitary operators

The projected bootstrap can reduce the CPU time needed to simulate the null distribution of goodness-of-fit statistics. At the same time, it is also possible to construct goodness-of-fit tests based on the asymptotically distribution-free transformation of empirical processes introduced in Khmaladze [2016]. If we do this, the limiting null distribution of the test statistics based on the transformed process will be known analytically and will not depend on the model we test. Such a feature is convenient for testing many different models simultaneously or when analyzing a large amount of data. For example, X-ray astronomical missions survey millions of astronomical sources. When analyzing the images and spectra arising from such observations, a common problem is identifying those in which features other than the background are present. In statistical terms, this problem involves testing spectral models on several millions of datasets, which would be unfeasible through case-by-case numerical simulations.

Given the prominence of the linear statistics, we consider the functions

$$\ell_t(x, z) = \frac{z - m_\theta(x)}{\sqrt{m_\theta(x)}} \mathbf{1}_{\{x \in A_t\}}$$

in which the sets A_t are members of the scanning family \mathcal{A} and are chosen so that

$$\mu(A_t) = t. \tag{44}$$

This condition is not necessary but simplifies the notation in what follows. Under (3) and if θ is known, the null distribution of the process $v_{\theta, \mathcal{K}}(\ell_t)$ converges weakly to that of a standard Brownian motion. When θ is estimated via MLE, $v_{\hat{\theta}, \mathcal{K}}(\ell_t)$ is asymptotically equivalent to $v_{\theta, \mathcal{K}}(\Pi \ell_t)$ and its limiting null distribution is that of a projected Brownian motion orthogonal to the score function s of the model we wish to test. Thus, the null distribution of test statistics based on $v_{\hat{\theta}, \mathcal{K}}(\ell_t)$ will be different for different models and for different values of θ within the same model.

However, it is possible to construct a linear operator in $\mathcal{L}_2(\mu_{\theta, \mathcal{K}})$, denoted by U_p , which maps the process $v_{\theta, \mathcal{K}}(\Pi \ell_t)$ into a process in t with standard distribution, unconnected with the model we are testing: the operator U_p will depend on the model, but the distribution of the resulting process will be free from it. In its spirit, the situation is not unlike the one encountered in the i.i.d. data regime in which the classical time-transformation $t = F(x)$ depends on the hypothetical F but maps F -empirical processes into the uniform empirical process, which is free from F .

The idea behind the choice of the operator U_p is geometrically clear: many different parametric models with a p -dimensional estimated parameter will asymptotically lead to projected Brownian motions parallel to the corresponding score functions. Therefore, the kernels of these projections, albeit different for different models, will all have the same dimension p . But then one can choose one such projection orthogonal to a fixed collection of p orthonormal functions and map particular projections corresponding to particular models into this chosen standard projection.

Let $r = \{r_j\}_{j=1}^p$ form a fixed orthonormal system in $\mathcal{L}_2(\mu_{\theta, \mathcal{K}})$. Unlike the coordinates of the orthonormalized score function $s = \{s_j\}_{j=1}^p$, this new system will stay the same for many different models. Consider the projection of ℓ_t orthogonal to r :

$$\Pi_r \ell_t(x, z) = \ell_t(x, z) - \sum_{j=1}^p \langle \ell_t, r_j \rangle r_j(x, z).$$

Choose U_p to be the unitary operator that maps r into s and, therefore, functions orthogonal to r into functions orthogonal to s . Then, the process $v_{\hat{\theta},K}(U_p\Pi_r\ell_t)$ serves our purpose since

$$v_{\hat{\theta},K}(U_p\Pi_r\ell_t) \sim v_{\theta,K}(\Pi U_p\Pi_r\ell_t) = v_{\theta,K}(U_p\Pi_r\ell_t)$$

and the variance of the process on the right-hand side – and, therefore, its covariance – depends on r but does not involve s :

$$E_{\theta}[v_{\hat{\theta},K}^2(U_p\Pi_r\ell_t)] = \|U_p\Pi_r\ell_t\|^2 = \|\Pi_r\ell_t\|^2 = \|\ell_t\|^2 - \sum_{j=1}^p \langle \ell_t, r_j \rangle^2. \quad (45)$$

Thus, the limiting distribution of statistics based on the transformed process $v_{\theta,K}(U_p\Pi_r\ell_t)$ will need to be found only once and then used for testing many different models.

Furthermore, we can suggest a particular choice of r that allows us to derive the asymptotic null distribution of goodness-of-fit statistics in closed form. For this, choose a sequence $\{A_{t_j}\}_{j=1}^p$ of sets within the scanning family \mathcal{A} such that $\mu(A_{t_j}) = j/p$. Denote with $\{B_j\}_{j=1}^p$ the collection of increments

$$B_j = A_{t_j} \setminus A_{t_{j-1}},$$

with $B_1 = \mathcal{X}$ if $p = 1$; for any p , $\{B_j\}_{j=1}^p$ provides an exhaustive partition of \mathcal{X} . Choose

$$r_j(x, z) = \frac{z - m_{\theta}(x)}{\sqrt{m_{\theta}(x)}} \sqrt{p} \mathbf{1}_{\{x \in B_j\}}. \quad (46)$$

We will see that, for this choice of r , the process $v_{\theta,K}(U_p\Pi_r\ell_t)$ is asymptotically a sequence of independent standard Brownian bridges.

One can split $\Pi_r\ell_t$ as the sum

$$\Pi_r\ell_t = \sum_{j=1}^p \ell_t \mathbf{1}_{\{x \in B_j\}} - \sum_{j=1}^p \langle r_j, \ell_t \rangle r_j = \sum_{j=1}^p [\ell_t \mathbf{1}_{\{x \in B_j\}} - \langle r_j, \ell_t \rangle r_j].$$

In this sum, only the summand for which $t_{j-1} < t \leq t_j$ is non-zero. For this summand

$$\|\ell_t \mathbf{1}_{\{x \in B_j\}}\|^2 \rightarrow t - t_{j-1}, \quad \text{while} \quad \langle r_j, \ell_t \rangle^2 \rightarrow p(t - t_{j-1})^2$$

and eventually, we obtain

$$E_{\theta}[v_{\hat{\theta},K}^2(U_p\Pi_r\ell_t)] \rightarrow t - t_{j-1} - p(t - t_{j-1})^2.$$

When comparing the last expression with the variance of the standard Brownian bridge $u(t)$, $t \in [0, 1]$, rescaled on the set B_j , i.e.,

$$u_j(t) = \frac{1}{\sqrt{p}} u(p(t - t_{j-1})), \quad t_{j-1} < t \leq t_j, \quad (47)$$

we find that they are the same. Therefore, asymptotically, the process $v_{\theta,K}(U_p\Pi_r\ell_t)$ is indeed a succession of rescaled independent standard Brownian bridges. For illustration purposes, one realization of such a process when $p = 4$ is provided on the right panel of Fig. 3.

The asymptotic null distribution of many goodness-of-fit statistics from such a process is analytically known. For example, consider

$$\text{KS}^* = \max_t |v_{\theta,K}(U_p\Pi_r\ell_t)|. \quad (48)$$

Since the maximum of a standard Brownian bridge is known to follow the Kolmogorov distribution [Kolmogorov, 1933], here denoted with $\mathcal{K}(\cdot)$, we have that, as $K \rightarrow \infty$,

$$P(\text{KS}^* \leq y | H_0) \rightarrow P\left(\max_i \left\{ \max_t |\sqrt{p} u_i(t)| \right\} \leq \sqrt{p} y\right) = \left[\mathcal{K}(\sqrt{p} y)\right]^p. \quad (49)$$

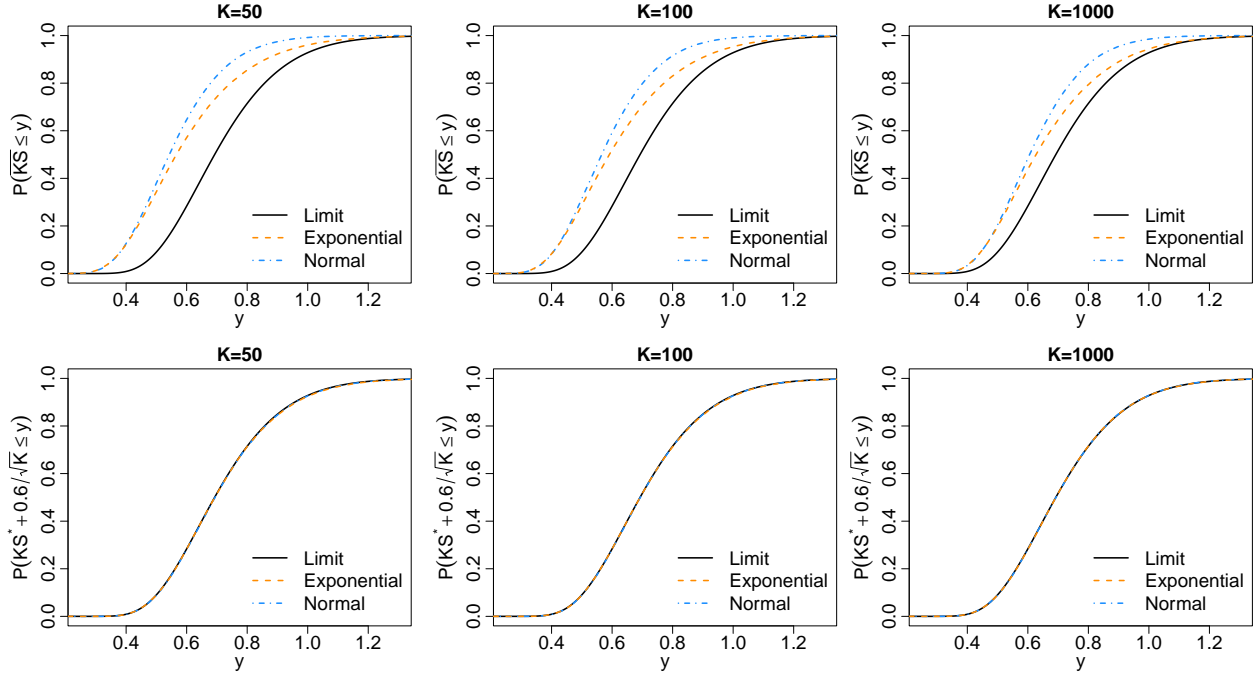


Fig. 4. Simulated null distributions of the test statistic \overline{KS} in (43) (top panels) and its transformed counterpart KS^* in (48) shifted by $\frac{0.6}{\sqrt{K}}$ (bottom panels), for the exponential (orange dashed lines) and the normal (blue chained lines) models for $K = 50, 100, 1000$. For comparison, the limiting distribution in (49) is also plotted in both panels (black solid lines). Each simulation has been conducted using 100,000 replicates.

The partial sums process, however, is observed over discrete times; hence, its maximum is always smaller than or equal to the maximum of the Brownian bridge, leading to a shift in the distribution. Nevertheless, the application of the continuity correction

$$\left[\mathcal{K}(\sqrt{p}(y + \frac{0.6}{\sqrt{K}})) \right]^p.$$

agrees with the finite- K distribution even for $K \sim 10$. A similar result can be obtained for situations in which the number of sets over which the partial sums are taken does not coincide with the number of bins.

It remains to address how to construct the unitary operator U_p . Consider the unitary operator $U_{a,b}$ defined as

$$U_{a,b} = I - \frac{\langle \cdot, a - b \rangle}{1 - \langle a, b \rangle} [a(x, z) - b(x, z)]$$

where $a, b \in \mathcal{L}_2(\mu_{\theta, K})$ and $\|a\| = \|b\| = 1$. $U_{a,b}$ maps a into b , b into a , and leaves functions orthogonal to both a and b unchanged. Proceed by constructing a set of auxiliary functions \tilde{r}_j such that $\tilde{r}_1 = r_1$ and, for $j > 1$, set

$$\tilde{r}_j(x, z) = U_{j-1} r_j(x, z) \quad \text{with} \quad U_j = U_{\tilde{r}_j, s_j} \dots U_{\tilde{r}_1, s_1}. \quad (50)$$

For example,

$$\tilde{r}_2(x, z) = U_{\tilde{r}_1, s_1} r_2(x, z), \quad \tilde{r}_3(x, z) = U_{\tilde{r}_2, s_2} U_{\tilde{r}_1, s_1} r_3(x, z), \quad \text{etc.}$$

Each function \tilde{r}_j is orthogonal to all s_i with $i < j$.

The operator U_p , constructed as in (50), is a product of unitary operators; hence, it is unitary, and it can be shown that $U_p r_j = s_j$ for all $j = 1, \dots, p$. Furthermore, given that Π_r and U_p are linear operators, $v_{\theta, K}(U_p \Pi_r \ell_t)$ is a function-parametric process with values given by weighted linear statistics. Thus, the corresponding $v_{\theta, K}(U_p \Pi_r \ell_t^\perp)$ component (cf. Section 6.4) is always zero.

Numerical study. To validate the performance of the approach described in this section in retrieving distribution-freeness, consider the exponential and normal models in Examples I and IV. In both instances, assume $\theta = (c, \beta)^\top$ to be unknown. Furthermore, to assess how large K needs to be for our asymptotic result to hold, we consider $K = 50, 100, 1000$. The top panels of Fig. 4 show the simulated null distributions of the statistic \overline{KS} in (43) with $g_\theta // \mathbb{1}_t = \ell_t$ and $t \in \{0, \frac{1}{K}, \frac{2}{K}, \dots, 1\}$. Due to the absence of distribution-freeness, regardless of how large K is, these null distributions differ substantially when testing the exponential model (orange dashed line) and the normal model (blue chained line). As expected, they also deviate from the limiting distribution in (49) (black solid lines). Conversely, the bottom panels of Fig. 4 show that, for all the values of K considered, the simulated null distributions of the KS^* in (48), adjusted by a factor of $\frac{0.6}{\sqrt{K}}$, is the same when testing either the exponential or the normal model. Moreover, both distributions coincide with the limit in (49).

8. Summary of the main results and final remarks

This article proposes a revision of the concept of divisible statistics that includes several forms of statistics routinely used in the analyses of grouped data and enables their representation as linear functionals of the random measure $v_{\theta, \kappa}(A, z)$. By studying the latter, researchers can acquire a comprehensive perspective on the behavior of the class of divisible statistics as a whole.

This study has revealed that, in a sparse regime, no single divisible statistic is adequate for goodness-of-fit; however, tests based on functionals of the partial sum process are. Moreover, parameter estimation can lead to higher power compared to testing for simple hypotheses. The most unexpected finding (for us) is that a class of weighted linear statistics dominates all divisible statistics.

We show that to conduct goodness-of-fit, it is beneficial to rely on omnibus functionals of the specific empirical process given in (42). Their null distribution can be efficiently derived using the projected parametric bootstrap. It is also possible to transform the empirical process to construct test statistics with an asymptotic null distribution free from the model and known in closed form.

The theoretical framework introduced in this manuscript is illustrated through the lenses of a Poisson-binned data analysis, it immediately applies to Poisson regression problems, and it naturally lends itself to any other situation in which non-identically distributed data are encountered. It would be interesting to explore extensions of the proposed setup to high-dimensional regression in which the size of parameter space is much larger than the sample size. Such a development could broaden further the set of inferential tools currently available in this context [e.g., [Chen and Lockhart, 2001](#), [van de Geer et al., 2014](#), [Janková et al., 2020](#)].

The application on data from the Chandra X-ray Observatory allowed us to detect departures from uniformity in X-ray source-free spectra. It also suggested that a revision of the linear model proposed by [Zhang et al. \[2023\]](#) may be needed to suitably describe the background distribution in the 14.6-17.4 Angstrom range.

Supplementary Material

Technical details, the R code, and the data needed to replicate the results presented in this manuscript are available in the Supplementary Material.

Acknowledgments

S.A. is grateful to the School of Mathematics and Statistics at the Victoria University of Wellington for providing the resources and fostering a welcoming environment at the beginning of this project. She also thanks Bob Cousins, Vinay Kashyap, Knut Morå, and Lawrence Rudnick for the useful discussions on goodness-of-fit problems arising in physics and astronomy. Both authors thank three anonymous referees and the editor for the thoughtful comments and constructive feedback.

Funding

This research is partially supported by the Office of the Vice President for Research at the University of Minnesota, by the NSF grant DMS-2152746, and the Marsden grant VUW1616.

References

- S. Algeri. K-2 rotated goodness-of-fit for multivariate data. *Physical Review D*, 105:035030, 2022.
- S.-i. Amari. *Differential-Geometrical Methods in Statistics*. Lecture Notes in Statistics. Springer, 1985.
- T. Anderson and D. Darling. A test of goodness of fit. *Journal of the American Statistical Association*, 49(268):765–769, 1954.
- W. B. Atwood et al. The Large Area Telescope on the Fermi Gamma-Ray Space Telescope Mission. *The Astrophysical Journal*, 697(2):1071, 2009.
- H. Baayen. *Word frequency distributions*. Kluwer, 2001.
- S. Balakrishnan and L. Wasserman. Hypothesis testing for high-dimensional multinomials: A selective review. *The Annals of Applied Statistics*, 12(2):727 – 749, 2018.
- S. Balakrishnan and L. Wasserman. Hypothesis testing for densities and high-dimensional multinomials. *The Annals of Statistics*, 47(4):1893–1927, 2019.
- A. Barbour and A. Gnedin. Small counts in the infinite occupancy scheme. *Electronic Journal of Probability*, 14:365–384, 2009.
- S. Belfonte et al. Search for resonant and nonresonant new phenomena in high-mass dilepton final states at $\sqrt{s} = 13$ TeV. *Journal of High Energy Physics*, 2021(07):1–62, 2021.
- M. Bonamente. Distribution of the c statistic with applications to the sample mean of poisson data. *Journal of Applied Statistics*, 47(11):2044–2065, 2020.
- T. T. Cai, Z. Ke, and P. Turner. Testing high-dimensional multinomials with applications to text analysis. *Journal of the Royal Statistical Society Series B: Statistical Methodology*, page qkae003, 2024.
- W. Cash. Parameter estimation in astronomy through application of the likelihood ratio. *Astrophysical Journal*, 228:939–947, 1979.
- G. Chen and R. Lockhart. Weak convergence of the empirical process of residuals in linear models with many parameters. *Annals of Statistics*, pages 748–762, 2001.
- D. Chibisov. An investigation of the asymptotic power of the tests of fit. *Theory of Probability and Its Applications*, 10(3):421–437, 1965.
- W. Cochran. The χ^2 test of goodness of fit. *The Annals of Mathematical Statistics*, 23(3):315–345, 1952.
- N. Cressie and T. Read. Multinomial goodness-of-fit tests. *Journal of the Royal Statistical Society: Series B (Methodological)*, 46(3):440–464, 1984.
- N. Cressie and T. Read. Pearson’s X^2 and the loglikelihood ratio statistic G^2 : A comparative review. *International Statistical Review*, 57(1):19–43, 1989.
- A. Danehkar, M. Karovska, J. Drake, and V. Kashyap. Long-term x-ray variability of the symbiotic system rt cru based on chandra spectroscopy. *Monthly Notices of the Royal Astronomical Society*, 2020.

- C. Domanski. Statistical tests based on empty cells. *Acta Universitatis Lodziensis*, (269), 2012.
- L. Dümbgen and J. Wellner. A new approach to tests and confidence bands for distribution functions. *The Annals of Statistics*, 51(1):260–289, 2023.
- A. Durio and Y. Y. Nikitin. Local efficiency of integrated goodness-of-fit tests under skew alternatives. *Statistics & Probability Letters*, 117:136–143, 2016.
- J. C. Gladstone, T. Roberts, and C. Done. The ultraluminous state. *Monthly Notices of the Royal Astronomical Society*, 397(4):1836–1851, 2009.
- A. Gnedin, B. Hansen, and J. Pitman. Notes on the occupancy problem with infinitely many boxes: general asymptotics and power laws. *Probability Surveys*, 4:146 – 171, 2007.
- N. Henze and S. Meintanis. Recent and classical tests for exponentiality: a partial review with comparisons. *Metrika*, 61:29–45, 2005.
- P. Humphrey and D. Buote. A Chandra view of the normal S0 galaxy NGC 1332. I. an unbroken, steep power-law luminosity function for the low-mass X-ray binary population. *The Astrophysical Journal*, 612(2):848, 2004.
- G. Ivchenko and Y. Medvedev. Separable statistics and hypothesis testing. the case of small samples. *Theory of Probability and Its Applications*, 23(4):764–775, 1979.
- G. Ivchenko and Y. Medvedev. Decomposable statistics and hypothesis testing for grouped data. *Theory of Probability and Its Applications*, 25(3):540–551, 1981.
- J. Janková, R. Shah, P. Bühlmann, and R. Samworth. Goodness-of-fit testing in high dimensional generalized linear models. *Journal of the Royal Statistical Society Series B: Statistical Methodology*, 82(3):773–795, 2020.
- M. Karovska, T. Gaetz, C. Carilli, W. Hack, J. Raymond, and N. Lee. A precessing jet in the ch cyg symbiotic system. *The Astrophysical Journal Letters*, 710(2):L132, 2010.
- R. Kass and P. Vos. *Geometrical Foundations of Asymptotic Inference*. John Wiley & Sons, 2011.
- A. Kenneth and R. Pyke. A uniform central limit theorem for set-indexed partial-sum processes with finite variance. *The Annals of Probability*, 14(2):582–597, 1986.
- E. Khmaladze. Martingale limit theorems for divisible statistics. *Theory of Probability and Its Applications*, 28(3):530–548, 1984.
- E. Khmaladze. Goodness of fit problem and scanning innovation martingales. *The Annals of Statistics*, 21(2):798–829, 1993.
- E. Khmaladze. Goodness of fit tests for “chimeric” alternatives. *Statistica Neerlandica*, 52(1):90–111, 1998.
- E. Khmaladze. Differentiation of sets in measure. *Journal of Mathematical Analysis and Applications*, 334(2):1055–1072, 2007.
- E. Khmaladze. Convergence properties in certain occupancy problems including the Karlin-Rouault law. *Journal of Applied Probability*, 48(4):1095–1113, 2011.
- E. Khmaladze. Unitary transformations, empirical processes and distribution free testing. *Bernoulli*, 22(1):563–588, 2016.
- E. Khmaladze and W. Weil. Local empirical processes near boundaries of convex bodies. *Annals of the Institute of Statistical Mathematics*, 60(4):813–842, 2008.

- A. Kolmogorov. Sulla determinazione empirica di una legge di distribuzione. *Giornale dell'Istituto Italiano degli Attuari*, 4:83–91, 1933.
- L. Le Cam. Locally asymptotically normal families of distributions. *University of California Publications in Statistics*, 3:37–98, 1960.
- E. Lehmann and J. Romano. *Testing statistical hypotheses*, volume 3. Springer, 1986.
- G. Luna and J. Sokoloski. The nature of the hard x-ray-emitting symbiotic star rt cru. *The Astrophysical Journal*, 671(1):741, 2007.
- A. Magurran. *Ecological Diversity and its Measurement*. Princeton University Press, 1988.
- H. Marlowe, P. Kaaret, C. Lang, H. Feng, F. Grise, N. Miller, D. Cseh, S. Corbel, and R. F. Mushotzky. Spectral state transitions of the ultraluminous X-ray source IC 342 X-1. *Monthly Notices of the Royal Astronomical Society*, 444(1):642–650, 2014.
- Y. Medvedev. Some theorems on the asymptotic distribution of the χ^2 statistic. *Doklady Akademii Nauk*, 192(5):987–989, 1970.
- S. Mirakhmedov. Asymptotic normality associated with generalized occupancy problems. *Statistics and Probability Letters*, 77(15):1549–1558, 2007.
- R. Mnatsakanov. A functional limit theorem for additively separable statistics in the case of very rare events. *Theory of Probability and Its Applications*, 30(3):622–626, 1986.
- R. Mnatsakanov. On the convergence of separable statistics to a Wiener process. *Theory of Probability and Its Applications*, 32(1):152–157, 1988.
- A. Moscovich, B. Nadler, and C. Spiegelman. On the exact Berk-Jones statistics and their p -value calculation. *Electronic Journal of Statistics*, 10(2):2329 – 2354, 2016. doi: 10.1214/16-EJS1172.
- U. Müller and G. Osius. Asymptotic normality of goodness-of-fit statistics for sparse Poisson data. *Statistics: A Journal of Theoretical and Applied Statistics*, 37(2):119–143, 2003.
- J. Oosterhoff and W. Van Zwet. A note on contiguity and Hellinger distance. *Reidel, Dordrecht*, 157: 166, 1979.
- K. Pearson. On the criterion that a given system of deviations from the probable in the case of a correlated system of variables is such that it can be reasonably supposed to have arisen from random sampling. *The London, Edinburgh, and Dublin Philosophical Magazine and Journal of Science*, 50 (302):157–175, 1900.
- R. Pyke. A uniform central limit theorem for partial-sum processes indexed by sets. *London Mathematical Society Lecture Notes Series*, 79:219–240, 1983.
- B. Roberts, J. Haywood, and E. Swordson. Distribution free testing for the family of laplace distributions. *Communications in Statistics-Simulation and Computation*, pages 1–12, 2023.
- W. Rudin. *Real and complex analysis*. McGraw-Hill, 1987.
- N. Smirnov. On the distribution of the von Mises ω^2 -criterion. *Matematicheskii Sbornik*, 5:973–993, 1937.
- N. Smirnov. On the estimation of the discrepancy between empirical curves of distribution for two independent samples. *Moscow University Mathematics Bulletin*, 2(2):3–14, 1939.
- S. Stigler. *The History of Statistics*. Harvard University Press, 1990.

- D. Swartz, S. Wolk, and A. Fruscione. Chandra's first decade of discovery. *Proceedings of the National Academy of Sciences*, 107(16):7127–7134, 2010.
- S. van de Geer, P. Bühlmann, Y. Ritov, and R. Dezeure. On asymptotically optimal confidence regions and tests for high-dimensional models. *The Annals of Statistics*, 42(3):1166 – 1202, 2014.
- A. van der Vaart. *Asymptotic Statistics*, volume 3. Cambridge University Press, 2000.
- J. Wellner. Empirical processes in action: a review. *International Statistical Review*, 60(3):247–269, 1992.
- X. Zhang, S. Algeri, V. Kashyap, and M. Karovska. A novel approach to detect line emission under high background in high-resolution x-ray spectra. *Monthly Notices of the Royal Astronomical Society*, 521(1):969–983, 2023.